Agricultural Systems 215 (2024) 103855

Contents lists available at ScienceDirect

Agricultural Systems

journal homepage: www.elsevier.com/locate/agsy

Multi-stakeholder multi-objective greenhouse design optimization

Xinyuan Min (闵心远)[a,*], Jaap Sok[a], Feije de Zwart[b], Alfons Oude Lansink[a]

[a] Business Economics, Wageningen University & Research, P.O. Box 8130, 6700 EW Wageningen, the Netherlands
[b] Wageningen Plant Research, Wageningen University & Research, P.O. Box 644, 6700AP Wageningen, the Netherlands

HIGHLIGHTS

- Greenhouse design needs to consider production, economic, and environmental interdependencies, and stakeholder preferences.
- We used bio-economic modelling, genetic algorithm, and a directional distance function approach to evaluate greenhouse designs.
- We identified several greenhouse designs with robust economic and environmental performances for four locations in China.
- Lighting system, structure, thermal screen, and CO_2 dosing rate were among the most influential factors on operating income.
- Lighting is the primary contributor to GHG emissions, while the use of thermal screens can effectively reduce GHG emissions.

GRAPHICAL ABSTRACT

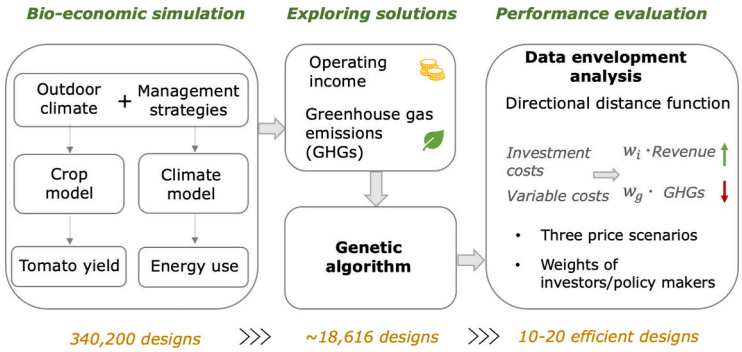

ARTICLE INFO

Original content: Multi-stakeholder multi-objective greenhouse design optimization (Original data)

Keywords:
Greenhouse design
Data envelopment analysis
Genetic algorithm
Bio-economic model
Multi-stakeholder

ABSTRACT

CONTEXT: Optimizing greenhouse design is a complex challenge that involves the large combinational solution space and the interactions between design elements, outdoor climate, and crops. In addition, evaluating greenhouse performance requires consideration of economic and environmental dimensions, as well as different stakeholder priorities.
OBJECTIVE: This study aims to identify greenhouse designs that are efficient in terms of economic and environmental performance for both policy makers and investors for four locations in China.
METHODS: This paper made a novel combination of operational research methods with bio-economic modelling. Specifically, a bio-economic model was used to simulate the yield, energy use, and economic and environmental performance of different greenhouse designs. A genetic algorithm was used to explore the large solution space to reduce the computational effort. The overall performance of greenhouse design was evaluated using a directional distance function approach, which incorporated stakeholders' priorities for economic and environmental performance through the directional vector.
RESULTS AND CONCLUSIONS: The results identify several greenhouse designs that were found to be efficient in terms of economic and environmental performance for both investors and policymakers across various price scenarios. The most influential factors on operating income include the choice of lighting, structure, thermal

* Corresponding author.
E-mail addresses: xinyuan.min@wur.nl (X. Min), jaap.sok@wur.nl (J. Sok), feije.dezwart@wur.nl (F. de Zwart), alfons.oudelansink@wur.nl (A. Oude Lansink).

https://doi.org/10.1016/j.agsy.2024.103855
Received 15 June 2023; Received in revised form 30 October 2023; Accepted 3 January 2024
Available online 20 January 2024

screen, and CO_2 dosing rate. Among lighting options, LED lighting outperforms HPS lighting in terms of both economic and environmental performance. Specifically, incorporating LED lamps with an intensity of 200 μmol m^{-2} s^{-1} can increase annual operating income by 97.3 to 200.2 ¥ m^{-2}, depending on the region. Conversely, low intensity lighting adversely impacts both economic and environmental performance. A synergistic relationship has been observed between lighting and CO_2 dosing. On the other hand, lighting is the primary contributor to greenhouse gas (GHG) emissions. Incorporating LED lighting with an intensity of 200 μmol m^{-2} s^{-1} can increase CO_2 equivalent emissions from 151.7 to 211.0 kg m^{-2}. Incorporating thermal screens can effectively reduce GHG emissions.

SIGNIFICANCE: The study presents an optimization approach that can be applied to various complex agricultural systems with interactions between many factors and the presence of multiple stakeholders with conflict priorities. In addition, our study has practical implications for the greenhouse sector in China. The wide range of optimal solutions provides policy makers and investors with the flexibility to choose greenhouse designs that meet regional agricultural development goals and budget constraints.

1. Introduction

China has the largest area of protected horticulture in the world, covering 1.89 million hectares (ha) by 2018 (Sun et al., 2019). However, China's protected horticulture is dominated by Chinese solar greenhouses[1] (66.6%) and single-span plastic tunnels (30.5%), which are typically small in size and have limited climate control capabilities. In comparison, large-scale modern greenhouse such as multi-tunnel plastic greenhouses or Venlo-type glasshouses, only make up 2.9% of China's protected horticulture area.

Promoting agricultural mechanization has become as a top priority of the Ministry of Agriculture (MOA) in China. Subsidies have stimulated a surge in investment in Venlo-type glasshouse in China (MOA, 2018). However, the economic returns of these investments were questionable (MOA, 2018). One explanation may be that the designs of these greenhouses were often imported directly from countries such as the Netherlands, without sufficient adaptation to the local climatic and market conditions in China. Identifying greenhouse designs that are optimally adapted to the local climate and market conditions in China is currently of high policy relevance.

Existing studies on greenhouse designs mostly address the design as a single factorial problem (e.g., Luo et al., 2005; Wang et al., 2014; Esmaeli and Roshandel, 2020), i.e., by optimizing one design element at a time. However, the design of greenhouse production systems is clearly a multi-factorial optimization problem (van Henten et al., 2006), requiring the selection of the best combination of design elements, such as the structure and cover material, the choice of heating system, screens, CO_2 supply, and artificial lighting. All of these choices mutually influence each other and are affected by local climate and market conditions (van Henten et al., 2006). A recent stream of literature advocates a more systematic approach, i.e., integrating the physical, biological, and economic models, and optimizing multiple factors simultaneously (e.g, Vanthoor et al., 2012; Naseer et al., 2021).

One of the methodological challenges of taking a systematic approach is the "curse of dimensionality"—the number of possible combinations increases exponentially with the number of design elements and the number of alternatives of each design element. Consequently, selecting the best combination of design options can be a complex task. Vanthoor et al. (2012) optimized the choice of greenhouse structure, cover material, shading and thermal screens, whitewash, heating and cooling system, CO_2 enrichment system for Spain and the Netherlands. Adopting the same modelling framework, Naseer et al. (2021) identified the optimal design for Norway among five predefined design alternatives.

Vanthoor et al. (2012) used the controlled random search method, which was originally developed for tackling continuous optimization problems (Price, 1977), to explore the solution space. However, the greenhouse design optimization problem is more suitable to be treated as a combinatorial optimization problem, as it involves discrete decisions regarding whether to include specific design element and which types to choose. In this regard, the genetic algorithm (GA) is an appropriate method (Holland, 1992). GAs fall under the category of evolutionary algorithms and are often used to generate solutions to search and optimization problems (Mendes et al., 2019). In agriculture, GAs have been applied to analyze problems such as farm management practices (Lehmann et al., 2013; Villalba et al., 2019), orchard replacement decisions (West, 2019), and food resource allocation problems (Notte et al., 2016).

A second component of optimal greenhouse design is the choice of criteria for evaluating the performance of different systems. Some scholars used biological or physical performance criteria, such as production levels (Luo et al., 2005) and the ability to maintain the indoor environment (Wang et al., 2014). Economic indicators are also well-accepted criteria for selecting the optimal greenhouse design (e.g., Vanthoor et al., 2012; Naseer et al., 2021). Apart from economic performance, environmental impact of greenhouse production is also an increasing concern for stakeholders, especially policy makers. Modern greenhouse production is associated with a high level of greenhouse gas (GHG) emissions due to the intensive use of energy. Different greenhouse designs have varying energy requirements, resulting in different environmental impacts (Zhou et al., 2021). Different stakeholders may assign different weights on the economic and environmental performance, and a greenhouse design that is ideal for investors may not be preferred by policy makers. The economic and environmental performance of different greenhouse designs have been compared in some studies (e.g., Naseer et al., 2022; Meyer-Aurich et al., 2012), but separately. However, for multi-stakeholder decision-making, the economic and environmental performance should be jointly assessed to achieve a form of consensus that reflects a trade-off between conflicting objectives and stakeholder priorities.

This study aims to identify greenhouse designs that are optimally adapted to the climate and market conditions for four different locations in China. The design elements considered are greenhouse structure, cover material, shading and thermal screens, heating and cooling systems, artificial lighting, CO_2 enrichment systems, and whitewash. In order to reduce the computational effort, a genetic algorithm was employed to explore the large solution space. To identify the designs that best fit stakeholders' preferences, a directional distance function approach was used to evaluate the overall performance of greenhouse designs in terms of economic and environmental performance. The optimal greenhouse designs were selected based on their ability to consistently deliver robust performance across different price scenarios. The resulting greenhouse designs were those where no improvement in economic performance can be achieved without compromising the

[1] The Chinese solar greenhouse features an arc-shaped south-facing, light-transmitting roof, and an energy-storing north wall. During the day, solar energy is collected through the roof and stored in the north wall and soil. The stored energy is released at night, with a thermal blanket applied to prevent energy loss. No additional heating is applied this type of greenhouse (Montero et al., 2019).

environmental performance, and vice versa.

The remainder of this paper is organized as follows: Section 2 presents the combination of methods used in this paper, i.e., the biophysical model for simulating greenhouse yield and energy use, the genetic search algorithm, and the directional distance function. This is followed by the description of the results in Section 3. The paper ends with Discussion and Conclusions.

2. Materials and methods

Fig. 1 presents the schematic overview of the combination of methods used in the greenhouse design optimization problem. A bioeconomic model was used to evaluate the economic and environmental performance of a given greenhouse design (Min et al., 2022). A genetic algorithm was used to explore the large combinational solution space, using economic performance as the fitness function. The search of genetic algorithm produced a subset of promising greenhouse designs, the overall performance of which were then evaluated by a directional distance function which aims at improving the economic performance and reducing environmental impacts simultaneously. The categorical regression was used to estimate the impact of individual design element alternatives on economic and environmental performance.

This study focuses on nine greenhouse design elements: 1) type of structure, 2) cover material, 3) presence, type, and capacity of cooling system, 4) capacity of heating system, 5) presence and type of thermal screen, 6) presence and type of shading screen, 7) presence, type, and intensity of artificial lighting system, 8) presence and capacity of CO_2 enrichment system, and 9) presence of whitewash. An overview of the alternatives of each design element is given in Table 1.

2.1. Bio-physical simulation of different greenhouse designs

This study uses a biophysical model INKTAM-KASPRO to simulate yield and energy use under different greenhouse designs. KASPRO is a dynamic greenhouse climate model that computes the greenhouse climate as a function of outdoor climate conditions and greenhouse climate management settings (De Zwart, 1996). The greenhouse climate computed by KASPRO is then fed into the tomato crop simulation model INTKAM to compute the daily gross photosynthesis and ultimately fruit weight (Marcelis et al., 2008). The inputs of the INKTAM-KASPRO are the greenhouse design configuration, outdoor climate, and the indoor climate management strategies. The outputs of the INKTAM-KASPRO are the monthly tomato yield, natural gas use, electricity use, and CO_2 use. The outputs of the biophysical model provided inputs for the evaluation of economic and environmental performance of a greenhouse design.

Four locations were considered: Jinshan (East China), Langfang (North China), Weifang (East China), and Pingliang (Northwest China). The outdoor climate differs significantly across regions, and this could impact the optimal cropping and heating schedules. Furthermore, variations in the climate from year to year can have a significant impact on the economic and environmental performances of a greenhouse (Vanthoor et al., 2012). However, it is computationally infeasible to run the simulation with climate data from every historical year. Therefore, the solution adopted was to use the long-term climate data with sufficient meteorological representativeness for a location. To achieve this, we constructed a typical meteorological year climate dataset for each location using the historical climate data from 2000 to 2020 obtained from the ERA5 climate dataset (Hersbach et al., 2018), following the method used by Song et al. (2007). The details of construction of the typical meteorological year climate dataset are presented in Appendix B. Table 2 displays the climate characteristics of each region based on the constructed typical meteorological year climate dataset.

For the greenhouse climate manage strategies, we obtained the temperature and screen use setpoints from two Chinese growers and a greenhouse consultant (K. Yang, personal communication, December 5, 2019; Y. Xie, personal communication, February 6, 2022; Y. Ying, personal communication, June 7, 2022). The CO_2 setpoint, which refers to the desired indoor CO_2 concentration, increases with the use of lights and deceases with the opening of vent. In practice, the growers adjust their climate management strategies daily in response to weather conditions. The dependencies between the climate setpoints and the weather conditions were captured by the proportional band parameter (Pband). The detailed greenhouse climate management strategy can be found in Appendix C. The same climate setpoints were applied across all four locations to ensure that any differences in design performance were solely attributed to local climate and market conditions.

2.2. Economic performance evaluation

The economic performance of a greenhouse design is defined as the annual operating income from greenhouse production:

$$\Pi = -EAC_{sum} + R_{tomato} - C_{var} \quad (1)$$

where Π (¥ m^{-2} $year^{-1}$) is the annual operating income from greenhouse production, R (¥ m^{-2} $year^{-1}$) is the annual revenue generated from harvested tomatoes, EAC_{sum} (¥ m^{-2} $year^{-1}$) is the annual fixed costs incurred from the depreciation and maintenance of greenhouse structure and equipment. C_{var} (¥ m^{-2} $year^{-1}$) is the variable costs of production.

Greenhouse structure and equipment have different life spans, and equipment replacement occurs at different times. To compare the fixed costs of different design elements with unequal lifetimes, the fixed costs associated with each design element was expressed as the Equivalent Annuity Cost (EAC). The total fixed costs of owning and maintaining the greenhouse is the sum of the EAC of each design element.

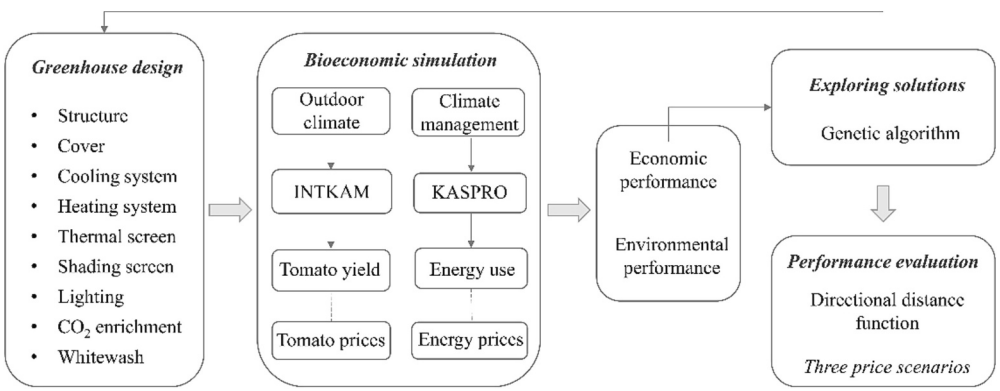

Fig. 1. Schematic overview of the greenhouse design optimization problem.

Table 1
Design element alternatives and associated economic parameters, encodings used for genetic algorithm.

Design elements choices	Investment ¥ m^{-2}	Investment ¥ $unit^{-1}$	Lifetime year	Maintenance % $year^{-1}$
Structure (i = 1)				
A: Multi-tunnel, 1 vent 10 m^{-2}	156.3 [g]	–	15 [a]	2% [a]
B: Multi- tunnel, 1 vent 20 m^{-2}	143.3 [g]	–	15 [a]	2% [a]
C: Multi- tunnel, 1 vent 30 m^{-2}	131.0 [g]	–	15 [a]	2% [a]
D: Venlo, 1 vent 10 m^{-2}	241.7 [g]	–	15 [a]	0.5% [a]
E: Venlo, 1 vent 20 m^{-2}	218.3 [g]	–	15 [a]	0.5% [a]
F: Venlo, 1 vent 30 m^{-2}	208.3 [g]	–	15 [a]	0.5% [a]
Cover (i = 2)				
A: PE (polyethylene) film	7.8 [g]	–	7 [a]	5% [a]
B: Double PE film	15.7 [g]	–	7 [a]	5% [a]
C: Glass	55.0 [g]	–	15 [a]	0.5% [a]
Cooling systems (i = 3)				
A: No				
B: Fogging: 200 g h^{-1} m^{-2}	25.6 [c]	–	10 [a]	5% [a]
C: Fogging: 300 g h^{-1} m^{-2}	29.1 [e]	–	10 [a]	5% [a]
D: Fogging: 400 g h^{-1} m^{-2}	46.5 [e]	–	10 [a]	5% [a]
E: Pad and fan: 60 m^3 h^{-1} m^{-2}	22.2 [e]	–	10 [a]	5% [a]
F: Pad and fan: 90 m^3 h^{-1} m^{-2}	27.5 [e]	–	10 [a]	5% [a]
G: Pad and fan: 120 m^3 h^{-1} m^{-2}	31.0 [c]	–	10 [a]	5% [a]
Heating system (i = 4)				
A: Boiler: 1.16 MW ha^{-1}	–	412,920 [e]	15 [a]	1% [a]
B: Boiler: 1.74 MW ha^{-1}	–	432,000 [e]	15 [a]	1% [a]
C: Boiler: 2.32 MW ha^{-1}	–	475,200 [e]	15 [a]	1% [a]
Thermal screen (i = 5)				
A: No				
B: a transparent woven screen with transmission of 72%	12 [b]	–	5 [a]	5% [a]
C: made of non-transparent bands woven with black and transparent threads. Both side of screens are white	18 [b]	–	5 [a]	5% [a]
D: a light blocking screen, white on one side and black on the other side	27.5 [b]	–	5 [a]	5% [a]
E: Double-layer, the top layer an aluminized screen, and the low layer a woven black screen	32.2 [e]	–	5 [a]	5% [a]
Structure for thermal screen	42 [b]	–	10 [e]	5% [e]
Shading screen (i = 6)				
A: No				
B: shading factor 36%	13.5 [b]	–	5 [a]	5% [a]
C: shading factor 45%	11 [b]	–	5 [a]	5% [a]
D: shading factor 56%	12 [b]	–	5 [a]	5% [a]
Structure for shading screen	42 [b]	–	10 [e]	5% [e]
Lighting (i = 7)				
A: No supplemental lighting				
HPS (High-pressure sodium) bulbs (2.3 μmol J^{-1}) B: 50 μmol m^{-2} s^{-1} C: 100 μmol m^{-2} s^{-1} D: 150 μmol m^{-2} s^{-1} E: 200 μmol m^{-2} s^{-1}		0.2 [a] ¥ W^{-1}	10,000 [a] hr	1% [a]
LED (light-emitting diode) lamp (3.1 μmol J^{-1}), F: 50 μmol m^{-2} s^{-1} G: 100 μmol m^{-2} s^{-1} H: 150 μmol m^{-2} s^{-1} I: 200 μmol m^{-2} s^{-1}	see Appendix A	4.2 [f] ¥ W^{-1}	35,000 [a] hr	0.5% [a]
HPS fixtures		0.9 [a] ¥ W^{-1}	7 [a]	1% [a]
Cabling		0.9 [a] ¥ W^{-1}	10 [a]	1% [a]
CO_2 enrichment (i = 8)				
A: no				
B: 50 kg CO_2 ha^{-1} h^{-1}				
C: 100 kg CO_2 ha^{-1} h^{-1}				
D: 150 kg CO_2 ha^{-1} h^{-1}				
E: 200 kg CO_2 ha^{-1} h^{-1}				
Pure CO_2 kg^{-1}	–	1[d]	–	–
CO_2 distribution system	3.7 [c]	–	10 [a]	5% [a]
Whitewash (i = 9)				
A: No				
B: 50% transmission	0.7 [e]	–	1	0

Note: The cost of the "Structure for thermal screen" is incurred only when thermal screen is incorporated. This rule also applies to the "Structure for shading screen", "HPS fixtures", "Cabling", and "CO_2 distribution system".
a Raaphorst et al. (2019)
b Greenhouse screen consultant (Y. Ying, personal communication, June 7, 2022)
c Construction budget of a tomato Venlo-type glasshouse in Shanghai, China.
d Greenhouse grower (Y. Xie, personal communication, July 19, 2022)
e Vanthoor et al. (2012)
f Supplemental lighting consultant (X. Chen, personal communication, Nov 26, 2022)
g Average costs provided by three greenhouse construction companies in China

$$EAC_i^j = \frac{I_i^j \bullet r}{1-(1+r)^{-n_i^j}} + I_i^j \bullet m_i^j \quad (2)$$

$$EAC_{sum} = \sum_{i=0}^{9} EAC_i^j \quad (3)$$

where EAC_i^j is the Equivalent Annuity Cost of design element i with alternative j. I_i^j (¥ m^{-2}) is the initial investment cost of design element i with alternative j. n_i^j is the lifetime of design element i with alternative j in years. r is the discount rate, calculated with the Weighted Average Cost of Capital method (see Appendix D). m_i^j (% $year^{-1}$) is a fixed percentage of the initial investment costs, reflecting the annual maintenance costs of design element i with alternative j. An overview of the initial investment costs and maintenance costs of the nine design elements can be found in Table 1.

The annual revenue R is the sum of the economic value of tomatoes produced in all months:

$$R = \sum_{t=1}^{12} P_{tomato}^t * Q_{tomato}^t \quad (4)$$

where P_{tomato}^t (¥ kg^{-1}) is the tomato price of month t. Q_{tomato}^t (kg m^{-2}) is the harvested tomato of month t.

Variable costs C_{var} is the sum of natural gas costs, electricity costs,

Table 2
Climate characteristics, cropping and heating schedules of four regions.

	Jinshan	Langfang	Weifang	Pingliang
Longitude	30°49′51.96″ N	39°30′34.99″ N	36° 42′ 24.39″ N	35°32′21.01″ N
Latitude	121°20′38.40″ E	116°41′40.99″ E	119° 9′ 42.33″ E	106°41′10.00″ E
Gross radiation of the year (MJ m^{-2})	5406.3	5764.3	5715.7	5593.3
Gross radiation in Dec, Jan, Feb (MJ m^{-2})	913.8	932	931.3	993.4
Average temperature in Jan (°C)	6.5	−3.7	−1.6	−2.7
Average temperature in Jul (°C)	28.7	27.5	27.4	22.9
Average humidity in Jul (%)	82.8	70.8	74.1	62.6
Transplanting date	Oct 1	Sep 15	Sep 15	Jan 1
Heating start date	Dec 1	Oct 25	Nov 5	Oct 10
Heating end date	Apr 20, next year	Apr 13, next year	Apr 20, next year	Apr 30
Final harvest date	Jul 1, next year	Jul 10, next year	Jul 10, next year	Dec 15
Weeks of production	39	43	43	50

CO_2 costs (if any), and other costs such as seedlings, material, fertilizer, crop protection, labour costs. The costs of natural gas was modelled on a monthly basis. C_{var} is given by:

$$C_{var} = \sum_{t=1}^{12} P_{gas}^{t} * Q_{gas}^{t} + P_{elec} * Q_{elec} + P_{CO_2} * Q_{CO_2} + C_{other} \quad (5)$$

where P_{gas}^{t} (¥ m^{-3}) is the natural gas price of month t. Q_{gas}^{t} (m^3 m^{-2}) is the natural gas use per unit area of month t. Annual heating costs is the sum of the product of P_{gas}^{t} and Q_{gas}^{t} of all months. Q_{elec} (kWh m^{-2} $year^{-1}$) is the electricity use for lighting and empowering other machineries. We used the average monthly price of liquid natural gas from 2017 to 2022, the longest period for which data are available, to represent the long-term natural gas price (Table E2, Appendix E).

Unlike liquid natural gas, the price of electricity in China is set by the government and has little variation from month to month. Therefore, a constant electricity price P_{elec} (¥ kWh^{-1}) was applied. The electricity price is 0.682 ¥ kWh^{-1} for Jinshan, 0.512 ¥ kWh^{-1} for Langfang, 0.525 ¥ kWh^{-1} for Weifang, and 0.439 ¥ kWh^{-1} for Pingliang. Q_{CO_2} is the amount of pure CO_2 (kg m^{-2} $year^{-1}$) supplied. P_{CO_2} (¥ kg^{-1}) represents the price of pure CO_2, which remains constant with no monthly variation. Labour use was divided into non-harvest labour and harvest labour, the latter was dependent on tomato yield. Variable costs not related to energy and labour use were assumed to be the same for all locations.

Monthly wholesale prices for cherry tomatoes in 2021 for each region were aggregated by taking the average price of several markets within the same region (Table E1, Appendix E). These price data do not differentiate between variety and quality differences between field-grown and greenhouse tomatoes. Greenhouse-grown tomatoes are marketed as premium agricultural products and can command higher prices due to their superior quality and brand recognition (Wang, 2020; Zhang et al., 2010). A price premium of 50% was added to the wholesale price to represent the prices of tomatoes produced in modern greenhouses.

2.3. Environmental performance evaluation

The environmental performance of a greenhouse design is a multi-dimensional construct that encompasses many aspects, such as the release of hazardous chemicals into water systems, water use efficiency, soil degradation, and GHG emissions to the atmosphere (Zhou et al., 2021). Assuming soilless cultivation and the same irrigation system for each greenhouse design, variations in the environmental performance of each design primarily stem from differences in GHG emissions from energy consumption (Torrellas et al., 2012). Therefore, to assess the environmental performance of greenhouse designs, GHG emissions from energy use during the cultivation phase were taken into account. Emissions from greenhouses construction, product storage and transportation were not included.[2] The three main types of GHGs considered were carbon dioxide (CO_2), methane (CH_4), and nitrous oxide (N_2O), which have varying effects on global warming. Emissions of each type of GHG were converted into CO_2 equivalent emissions using specific global warming potentials (GWPs), as shown in Table 3. The environmental impact of a greenhouse design was computed using eq. (6):

$$E = \sum_{GHG} \left(Q_{gas} * e_{gas} * GWP_{gas} \right) + Q_{elec} * e_{elec} \quad (6)$$

where E (kg m^{-2}) is the total amount of CO_2 equivalent emissions per unit area. Q_{gas} (m^3 m^{-2}) and Q_{elec} (kWh m^{-2}) are the annual consumption of natural gas and electricity per unit area. e_{gas} is the emission factor of natural gas (liquids) for the specified type of greenhouse gas. GWP_{gas} (CO_2e kg^{-1}) is the global warming potentials for the specified type of greenhouse gas. The emission factor of purchased electricity e_{elec} differs by region, depending on the proportion of electricity generated from renewable energy sources in the regional grid (Qu et al., 2017). Table 3 shows the emission factors of liquid natural gas and electricity.

2.4. Search strategy – Genetic algorithm

For the given set of design elements, the number of possible design alternatives would be equal to 340,200. A simulation for one design takes 20 s; hence, exploring all design alternatives would take 197 days,

Table 3
Emission factors for greenhouse gases emissions from energy use in greenhouse production.

Energy type	GHG type	Emission factor	Unit	GWP
Liquid natural gas	CO_2	64,200 [a]	kg TJ^{-1}	1
	CH_4	10 [a]	kg TJ^{-1}	28 [b]
	NO_2	0.6 [a]	kg TJ^{-1}	265 [b]
Electricity	CO_2e	Langfang: 0.9236 [c] Weifang: 0.8007 [c] Jinshan: 0.6392 [c] Pingliang: 0.5312 [c]	kg kWh^{-1}	1

a. Source: IPCC (2007), volume 2, Chapter 2, Table 2.5.
b. Source: IPCC (2014), Box 3.2, Table 1, with time horizon for 100 years.
c. Source: Qu et al. (2017).
Note: net calorific value of liquid natural gas: 51434 MJ ton^{-1}. Net calorific value of natural gas: 38.931 MJ m^{-3}. One ton of liquid natural gas was converted to 1320 m^3 of natural gas.

[2] The GHG emission reporting guidelines for facility agriculture enterprises in China do not require reporting emissions from the construction and transportation phases. The guidelines specify the scope of the GHG assessment to include fossil fuel consumption, purchased electricity, and chemical use for greenhouse cultivation activities. Consequently, emissions related to other stages are of lesser concern to investors and policy makers in China.

and this number is multiplied by four as we would like to explore the optimal design for four locations. Given this enormous computational time, it is impractical to simulate all design alternatives for each location. To ease the computational effort, a genetic algorithm (GA), an adaptive heuristic search algorithm based on Darwinian natural selection (Aytug et al., 2003; Mayer et al., 1999), was employed to search for close-to-optimal designs.

GA has five basic components: 1) a genetic representation of solutions (in this case, the representation of greenhouse designs) to the problem, 2) A way to generate an initial population of solutions, 3) an evaluation function to calculate the fitness score of solutions, 4) crossover and mutation operators to alter the genetic composition of offsprings during reproduction, and 5) Values for the parameters of GA (Zbigniew, 1996). The steps of genetic algorithm are:

1. *Initialization*. Define N, the size of population. Randomly generate N design strings as the *initial population*.
2. Define the *initial population* as the *current population*.

   Initialize $Counter = 0$.

3. Define the termination condition, the maximum number of iterations $Counter_{max}$.

   While $Counter < Counter_{max}$:

4. *Evaluation*. Calculate the economic and environmental performances of each design in the *current population*.
5. *Selection*. Randomly draw two design strings from the current population, select the design string with the higher economic performance to enter the *parent pool* (binary tournament selection). Repeat this process until the size of *parent pool* reaches N.
6. *Crossover*. Each string in the *parent pool* has a probability of $P_{crossover}$ of being removed from the *parent pool* and selected to enter the *mating pool*. Randomly choose two strings from the *mating pool* as the parent chromosomes. Select two crossover points at random and swap the bits of parent chromosomes between the two points, resulting two offspring chromosomes. The offspring chromosomes and the remaining members of the *parent pool* together constitute the *population after crossover*.
7. *Mutation*. The mutation operator randomly changes any position of the string to a random different letter with a probability of P_{mutate}. After applying the mutation operator for each design string in the *population after crossover*, we obtain the *population after mutation*.
8. Update the *population after mutation* as the *current population*. Update the string with the highest economic performance as the *best string*.
9. Iteratively execute steps 5 to 9 until meeting the stopping criteria ($Counter = Counter_{max}$).

A key step of GAs is to encode a solution of a real-world problem into a chromosome. GA was originally encoded as binary strings, however in the real world, especially the field of engineering, many problems cannot be represented with binary encoding (Gen and Cheng, 1999). This holds true for the greenhouse design optimization problem, as each design component consists of more than two design options. Therefore, we used literal permutation encoding to represent a greenhouse design as a string of nine letters, where each letter represents a design element and its corresponding option. The index of the design component and the letter representation of the options are given in.

Table 1. One example of a design string is *DCBABAABA*, which represents a Venlo-glasshouse with one vent per 10 m^2 floor area, a fogging system with the capacity of 200 g h^{-1} m^{-2}, a boiler with heating capacity of 1.16 MW ha^{-1}, transparent thermal screens (transmissivity 72%), no shading screen, HPS lamps with light intensity of 50 μmol m^{-2} s^{-1}, CO_2 enrichment system at a dosing rate of 50 kg CO_2 ha^{-1} h^{-1}, no whitewash applied. Glass cover is infeasible for multi-tunnel structure, and PE film cover are considered for Venlo-type structure. Thus the strings with $i_1 = \{A, B, C\}$ and $i_2 = C$, or $i_1 = \{D, E, F\}$ and $i_2 = \{A, B\}$ are infeasible solutions and should be removed from the solution space. During the iterations of GA, the infeasible design strings were always converted to feasible ones.

The choice of population size, crossover and mutation probabilities is critical to the efficiency of GA. A small population size could lead the algorithm to provide poor solutions, while a too large population size would require more computation time to find a good solution (Diaz-Gomez and Hougen, 2007). In general, the suitable population size should be proportional to the number of dimensions of the problem (Harik and Lobo, 1999). A good balance between the crossover and mutation probabilities could direct the search towards promising regions, while maintaining the degree of diversity in the population, to avoid premature convergence (Harik and Lobo, 1999). Usually, the values for these parameters are chosen empirically for the specific class of optimization problems (Eremeev, 1999). After experimenting with a number of parameter combinations, we chose $N = 400, P_{crossover} = 0.5$, $P_{mutate=}0.1$, $Counter_{max} = 60$.

2.5. Overall performance evaluation - the directional distance function approach

We used the directional distance function approach to evaluate the overall performance of greenhouse production systems in terms of the revenues and GHG emissions generated. Following Chung et al. (1997), under the hypothesis of variable rate of return to scale, the directional distance function is defined as $\overrightarrow{D}\left(EAC_{sum}, C_{var}, \mathrm{R}, \mathrm{E}; \overrightarrow{d}\right)$, The two types of inputs are EAC_{sum} and C_{var}. The two types of outputs are the (desired) annual revenue and the (undesired) GHG emissions of production. $\overrightarrow{d}$ is the directional vector, defined as $\overrightarrow{d} = \left(w^{R}_{stakeholder}{}^{*}\mathrm{R}_0, -w^{GHG}_{stakeholder}{}^{*}E_0\right)$, where $w^{R}_{stakeholder}$, $w^{GHG}_{stakeholder}$ represent the relative importance (weights) of revenue increase and environmental impacts reduction in the view of the stakeholders (investors or policy makers). This choice of directional vector implies that for given levels of inputs, the stakeholder aims at simultaneously increasing revenue at the rate of $w^{R}_{stakeholder}$, and decreasing GHG emissions at the rate of $w^{GHG}_{stakeholder}$.

The values for w^R and w^{GHG} are 0.86 and 0.14 for investors, and 0.7 and 0.3 for policy makers. These values are the averaged relative importance of economic and environmental performance according to ten greenhouse investors and policy makers. The values were obtained through a survey with the stakeholders and calculated by using the Best-Worst method (Unpublished results of Min et al., see Appendix F).

The measure of inefficiency β can be calculated as solutions to the following linear programming problems:

$$max\beta \tag{7}$$

$$\text{s.t.} \sum \lambda_k EAC_{sum} \leq EAC_{i0} \tag{8}$$

$$\sum \lambda_k C_{var_k} \leq C_{var_0} \tag{9}$$

$$\sum \lambda_k \mathrm{R}_k \geq \mathrm{R}_0 + \beta^{*} w^{econ}_{stakeholder}{}^{*}\mathrm{R}_0 \tag{10}$$

$$\sum \lambda_k \mathrm{GHG}_k \leq \mathrm{GHG}_0 - \beta^{*} w^{env}_{stakeholder} GHG_0 \tag{11}$$

$$\sum \lambda_k = 1 \tag{12}$$

$$\lambda_k \geq 0, k = 1, \ldots, K; \beta \geq 0 \tag{13}$$

A greenhouse design is considered to be fully efficient when β takes the value zero.

2.6. Scenario analysis – find out robust greenhouse designs

The profitability of greenhouse production faces uncertainty due to fluctuating input and output prices. A greenhouse system that is considered optimal based on a given set of prices may not remain optimal for other price scenarios. A good greenhouse design should possess resilience and deliver robust performance in a dynamic market environment. To find out greenhouse designs that are robust to different price settings, we conceived three price scenarios: the baseline scenario, the low tomato price scenario, and the high energy cost scenario. The baseline scenario used 2021 tomato and energy prices as inputs for the simulation. The low tomato price scenario assumed a 30% reduction in tomato prices compared to the baseline scenario. In the high energy cost scenario, both gas and electricity prices were assumed to be 20% higher than the 2021 levels.

For each price scenario, we calculated the inefficiency scores β for both investors (β_{invest}) and policy makers (β_{policy}), which produced an approximation of the efficiency frontier. Designs with $\beta_{invest} = \beta_{policy} = 0$ were considered efficient for that specific price scenario. Greenhouse designs that were found to be efficient across all three price scenarios were considered robust.

To explore the relationship between the design elements and annual operating income or GHG emissions (under the baseline scenario), we performed categorical regression analyses. The interaction terms between the level-specific lighting and CO_2 dosing choices were included, as CO_2 enrichment and supplemental lighting were found to have a synergistic effect in increasing the light use efficiency of crops (Heuvelink et al., 2018). A positive coefficient indicates that, ceteris paribus, selecting the specific design element leads to a higher operating income than the baseline choice. Conversely, a negative coefficient indicates a lower operating income compared to the baseline choice.

3. Results

For each location, the genetic search examined between 11,195 and 18,616 greenhouse designs, which represented 3.3% to 5.5% of all possible designs. Section 3.1 and 3.2 present the top five efficient designs based on economic and environmental performance, respectively, for each location. Results of the categorical regression for the operating income and GHG emissions are reported in Section 3.3 and 3.4, respectively.

3.1. Efficient greenhouse designs with the highest operating income

Table 4 presents the five efficient designs with the highest operating income in the baseline scenario for each location. The differences in profit per m^2 between the five designs are small, but with an average-sized greenhouse size of 1.5 ha, the cumulative difference can be large.

For Jinshan, a Venlo-type structure with glass cover was found to be the most favorable choice. A small-capacity boiler (1.16 MW ha^{-1}) and thermal screen with moderate energy-saving but high transmissivity was always selected. No cooling system or shading screen was chosen among the three efficient designs with the highest operating income in the baseline scenario. LED lamps with a high light intensity (200 μmol m^{-2} s^{-1}) coupled with CO_2 dosing at rate above 100 kg ha^{-1} h^{-1} were selected. Whitewash was selected only once out of the five efficient designs.

For Langfang, the recommended structure and cover were either a multi-tunnel structure with single PE film or a Venlo-type structure with glass cover. Given the cold winters in Langfang, it was suggested to opt for a high-capacity boiler (2.23 MW ha^{-1}) along with double-layer thermal screens. All efficient designs had LED lamps with high light intensity and the maximum CO_2 dosing rate, as well as whitewash.

For Weifang, a multi-tunnel structure and shading screens with a shading level of 36% were selected in three out of the five listed designs.

Table 4
Simulation results per m^2 of the efficient greenhouse designs with the highest operating income for each location.

Design element choice									Simulation outcome				
ST	CV	FG	HT	TS	SS	LT	CO_2	WW	***EAC***	***R***	C_{var}	***Π***	***GHG***
Jinshan													
Venlo	Glass	No	1.16	Transp	No	LED 200	200	No	81	543	243	223	118
Venlo	Glass	No	1.16	Transp	No	LED 200	200	Yes	83	546	247	220	121
Venlo	Glass	No	1.16	Transp	No	LED 200	100	No	81	529	235	217	118
Venlo	Glass	200	1.16	Transp	36%	LED 200	200	No	99	540	234	211	114
Venlo	Glass	300	1.16	Transp	36%	LED 200	150	No	98	533	231	209	115
Langfang													
MT	S-PE	No	2.23	D-layer	36%	LED 200	200	Yes	91	751	256	405	184
MT	S-PE	300	2.23	Transp	No	LED 200	200	Yes	77	745	264	405	176
Venlo	Glass	200	2.23	D-layer	36%	LED 200	200	Yes	107	760	252	403	182
Venlo	Glass	300	2.23	D-layer	36%	LED 200	200	Yes	107	761	252	403	182
MT	S-PE	200	2.23	D-layer	No	LED 200	200	Yes	84	753	267	403	182
Weifang													
MT	D-PE	No	1.16	D-layer	36%	LED 200	200	No	92	502	243	168	161
MT	S-PE	No	2.23	Transp	36%	LED 200	200	No	81	495	248	167	146
MT	S-PE	No	1.74	Transp	36%	LED 200	200	No	80	495	348	167	147
Venlo	Glass	200	2.23	Transp	No	LED 200	200	No	84	502	251	167	146
Venlo	Glass	300	2.23	Transp	No	LED 200	200	No	85	502	251	166	146
Pingliang													
MT	S-PE	No	1.16	Transp	No	LED 200	200	No	72	795	214	511	115
Venlo	Glass	200	2.23	Transp	36%	LED 200	200	No	100	814	208	507	112
Venlo	Glass	No	1.16	Transp	36%	LED 200	200	No	94	807	206	507	112
Venlo	Glass	300	2.23	Transp	36%	LED 200	200	No	100	814	208	507	112
MT	D-PE	200	1.74	D-layer	36%	LED 200	200	No	100	816	211	506	123

ST stands for structure, *MT* stands for multi-tunnel, *CV* stands for cover, *FG* stands for fogging, *HT* stands for heating capacity, *TS* stands for thermal screen, *SS* stands for shading screen, *LT* stands for lighting, *CO_2* stands for CO_2 enrichment, *WW* stands for whitewash. *S-PE* stands for Single PE. *D-PE* stands for Double PE. *Transp* stands for Transparent. *D-layer* stands for Double layer.

When using single PE film as the cover material, which has higher transmissivity than double PE film, the transparent thermal screens were recommended. This choice of cover material and thermal screen aimed to increase light use efficiency and maximize yield. On the other hand, when double PE film, which has better insulation but less transmissivity than single PE film, was selected, the recommended design consisted of a small-capacity boiler and double-layer thermal screen with excellent insulation but no transmissivity, with the focus on maximizing energy savings and reducing variable costs. Similar cover and thermal screen combinations were recommended for Pingliang, with glass or single PE film coupled with transparent thermal screens, and double PE film coupled with double-layer screens. For Weifang, LED lamps with high light intensity were selected, together with CO_2 dosing rate at 200 kg ha^{-1} h^{-1}. No whitewash was applied in the listed designs.

For Pingliang, the efficient design with the highest operating income in the baseline scenario was a relatively low-cost multi-tunnel structure with single PE film, without cooling system, shading screen or whitewash. LED lamps with the highest light intensity and a CO_2 enrichment system at the highest dosing rate were always present among the five listed designs.

3.2. Efficient greenhouse designs with the lowest greenhouse gas emissions

Table 5 displays the top five efficient designs with the lowest GHG for each location, under the condition of a positive operating income in all three price scenarios. None of the designs with the best environmental performance for Langfang and Pingliang included supplemental lighting. However, LED lamps with an intensity of 200 μmol m^{-2} s^{-1} were necessary, in order to maintain positive operating income across all price scenarios for Jinshan and Weifang.

Unlike the five efficient designs in Table 4 for Langfang, which favored double-layer thermal screens, transparent thermal screens were selected when ranked on environmental performance. Conversely, most of the designs for Pingliang in Table 4 selected transparent thermal screens, but double-layer thermal screens became the preferred option when ranked on environmental performance. There are trade-offs between economic and environmental performance, and generally, GHG increase with operating income.

3.3. Relationship between the design element choice and operating income

The results of the categorical regression analysis on operating income are shown in Table G1 in Appendix G. Almost all parameters were significant at the 0.05 critical level, as could be expected for this number of observations. The analysis indicates that the choices of lighting system, structure, thermal screen, and CO_2 dosing rate were the most influential factors on the operating income. In contrast, the choices of cover material, boiler capacity, shading screen, and whitewash had relatively small impacts on the operating income of a tomato greenhouse.

A structure with lower vent area was more favorable across all locations. Using double PE film as the cover material reduced the operating income in Jinshan and Langfang but increased it in Weifang and Pingliang. A pad and fan cooling system was not suitable for a tomato greenhouse, as indicated by the negative coefficients for each location. A fogging system was economically beneficial only for Langfang. A boiler with a capacity of 1.16 MW ha^{-1} was the preferred choice for Jinshan and Weifang, while a capacity above 1.74 MW ha^{-1} was preferable for Langfang and Pingliang. Overall, the choice of boiler capacity had limited impact on the operating income. All types of thermal screens, compared to no thermal screen, significantly increased the operating income of a tomato greenhouse. The transparent and double-layer thermal screens were the most effective measures for increasing operating income. The presence of shading screens slightly decreased the

Table 5
Simulation results per m^2 of the efficient greenhouse designs with the lowest GHG for each location, under the condition of positive operating income in all price scenarios.

Design element choice									Simulation outcome				
ST	CV	FG	HT	TS	SS	LT	CO_2	WW	***EAC***	***R***	C_{var}	***II***	***GHG***
Jinshan													
Venlo	Glass	300	1.16	Transp	36%	LED 200	200	No	99	540	234	211	114.4
Venlo	Glass	300	1.16	Transp	36%	LED 200	150	No	99	533	231	208	114.4
Venlo	Glass	No	1.16	Transp	36%	LED 200	100	No	93	521	227	206	114.4
Venlo	Glass	200	1.16	Transp	36%	LED 200	150	No	98	533	231	209	114.5
Venlo	Glass	400	1.74	Transp	36%	LED 200	200	No	102	541	235	208	114.9
Langfang													
MT	D-PE	200	1.16	Transp	No	No	No	No	41	305	166	99	63.3
MT	D-PE	400	1.16	Transp	No	No	100	Yes	46	316	171	98	63.3
MT	D-PE	200	1.16	Transp	No	No	200	Yes	42	319	174	102	63.4
MT	S-PE	No	1.74	Transp	No	No	100	Yes	36	322	184	103	69.5
MT	S-PE	No	1.74	Transp	No	No	150	Yes	36	323	185	102	69.6
Weifang													
Venlo	Glass	No	1.16	Transp	36%	LED 200	50	No	91	467	227	150	142.1
Venlo	Glass	300	1.16	Transp	36%	LED 200	100	No	96	481	233	153	142.4
Venlo	Glass	No	1.16	Transp	36%	LED 200	150	No	91	488	236	162	142.4
Venlo	Glass	300	1.16	Transp	36%	LED 200	150	No	96	490	237	157	142.5
Venlo	Glass	400	1.16	Transp	36%	LED 200	100	No	100	482	233	151	142.5
Pingliang													
MT	D-PE	300	1.74	D-layer	45%	No	No	No	58	292	117	117	41.2
MT	D-PE	No	2.23	D-layer	No	No	150	Yes	44	300	126	130	41.5
MT	D-PE	No	1.16	D-layer	No	No	150	Yes	43	295	126	125	41.5
MT	D-PE	200	1.16	D-layer	No	No	100	No	47	301	125	129	41.6
MT	D-PE	300	1.16	D-layer	No	No	200	No	48	302	128	127	41.6

ST stands for structure, *MT* stands for multi-tunnel, *CV* stands for cover, *FG* stands for fogging, *HT* stands for heating capacity, *TS* stands for thermal screen, *SS* stands for shading screen, *LT* stands for lighting, *CO_2* stands for CO_2 enrichment, *WW* stands for whitewash. *S-PE* stands for Single PE. *D-PE* stands for Double PE. *Transp* stands for Transparent. *D-layer* stands for Double layer.

operating income of a tomato greenhouse in Jinshan, while shading screens with a 36% shading factor was the best choice for the other locations.

LED lamp with an intensity of 200 μmol m^{-2} s^{-1} was found to be the optimal lighting solution for all locations. LED lamp almost always outperformed HPS lamps given the same light intensity. The operating income in Jinshan, Langfang, and Weifang significantly decreased when the light intensity fell below 100 μmol m^{-2} s^{-1}. CO_2 enrichment without the presence of supplemental lighting was only profitable for Pingliang. The significance and magnitude of the interaction term coefficients between lighting and CO_2 dosing rate indicated a synergistic effect between lighting and CO_2 enrichment. However, the synergistic effect was negative for Pingliang when a low light intensity (below 100 μmol m^{-2} s^{-1}) was applied. The combination of a high light intensity (200 μmol m^{-2} s^{-1}) and a high CO_2 dosing rate (200 kg CO_2 ha^{-1} h^{-1}) showed the best ability to improve operating income.

3.4. Relationship between the design element choice and GHG

Table G2 in Appendix G presents the regression results regarding the effect of individual design elements on GHG emissions. The results indicates that lighting was the primary contributor to GHG emissions. Compared to HPS lamp, using LED lamp produces less GHG emissions. Additionally, incorporating thermal screens can effectively reduce GHG emissions, particularly when utilizing transparent or double-layer thermal screens. Furthermore, greenhouse with smaller vent areas were found to generate fewer GHG emissions. In particular, the Venlo-type structure was found to contribute less to GHG emissions compared to multi-tunnel structure with the same vent area. Although double PE film offers better heat insulation, using it as the cover material slightly increased GHG emissions. This may be attributed to the reduction in light penetration, which can lead to longer lighting hours. Lastly, fogging capacity, boiler capacity, shading screen, CO_2 enrichment, and whitewash were found to have little impact on GHG emissions.

4. Discussion

The optimization of greenhouse design is complex as it involves the large combinational solution space and the interrelations between design elements, outdoor climate, and crops. This study demonstrates how a novel combination of operational research methods together with bio-economic modelling can effectively address the challenge of greenhouse design optimization. By coupling a genetic algorithm with a bio-economic greenhouse model, the solution space was reduced to 3% to 5% of the entire design space. The use a directional distance function approach for performance evaluation allows us to identify a range of designs that are located on the efficiency frontier, rather than a single optimal solution.

This study extends existing work on greenhouse design optimization in several ways. Previously, Vanthoor et al. (2012) focused solely on optimizing greenhouse designs based on economic performance. Torrellas et al. (2012) and Naseer et al. (2022) evaluated both economic and environmental aspects of various greenhouse designs separately, without considering the trade-offs between them. Our study contributes to this field by optimizing greenhouse designs from both aspects, taking into account multiple stakeholders' preference. This approach enables us to identify solutions that are acceptable to both investors and policy makers. Furthermore, the impact of price uncertainty is often overlooked in previous studies. While a greenhouse design may be considered optimal under a given set of prices and costs, it may not remain optimal under different price scenarios. To address this, we accounted for price uncertainty by selecting designs that were robust (i.e., optimal) under different price scenarios.

Our results clearly indicate that different regions require distinct greenhouse designs tailored to local climate and market conditions. Based on the findings of our study, Chinese policy makers can design region-specific subsidy policies to support technologies that are well-suited for individual regions, rather than subsidizing a broad range of technologies. For instance, the Venlo-type glasshouse was the most suitable structure for Jinshan. Double-layer thermal screens are advantageous in colder regions such as Langfang for energy-saving purposes. Moreover, LED lighting and CO_2 enrichment should be promoted as a bundled technology due to their synergistic effect on enhancing economic returns. Our findings can also help Chinese investors to make more informed investment decisions. Investors could flexibly select suitable designs based on their available budget or other relevant factors among the identified optimal greenhouse designs.

Our approach can be applied to many real-world problems, particularly those embedded in complex systems with interactions between factors, where establishing analytical relationships between decision variables and performance measures is difficult. These types of problems often have multiple (and often conflicting) objectives, and simulating such systems can be time-consuming. Previous efforts have combined DEA with GA to address challenges such as supplier selection (Shadkam and Bijari, 2017), agricultural production (Whittaker et al., 2009), resource allocation in hospitals (Lin et al., 2013), and aircraft spare parts allocation (Lee et al., 2008). However, none of these approaches considered the presence of multiple stakeholders, whose weights for different objectives may differ. Therefore, our approach represents an advancement in this research domain.

Some further issues can be studied in future research. Firstly, it should be noted that this study employed the same greenhouse climate setpoints across all price scenarios. In reality, the optimal climate setpoints may vary depending on the price levels, and greenhouse growers may adjust climate setpoints with changes in energy prices (Los et al., 2021). Therefore, a model that optimizes greenhouse design and climate management simultaneously is worth further exploration. A bilevel optimization formulation may be well-suited to this context.

Secondly, the study used typical meteorological year climate data as inputs for its analysis. The typical meteorological year climate data was constructed based on climate data from 2000 to 2020. This implies that greenhouse designs were optimized to adapt to past climate conditions. However, in the context of climate change, it is also possible to take a forward-looking perspective and optimize greenhouse designs based on projected climate conditions for the next 20 years.

Weather conditions can vary greatly from year to year, affecting yield, energy use, and operating income. Different greenhouse designs may respond differently to weather uncertainties. For instance, a greenhouse design with excellent heat insulation may not produce the best economic outcome in a typical climate year but could potentially yield better results during an extremely cold year. Therefore, instead of focusing on typical climate conditions, it may be valuable to consider the production risk arising from weather uncertainty and examine the distribution of the economic outcomes. In this case, a robust optimization approach could be suitable.

Thirdly, it is worth mentioning that the environmental performance assessment in this study focused solely on GHG emissions generated from energy use. However, it should be acknowledged that the GHG emissions generated from the construction phase of different greenhouse designs can vary greatly. To calculate the emissions related to greenhouse construction, we would need detailed data on the materials and quantities associated with the design alternatives listed in Table 1. Unfortunately, such detailed information was not available. For a fairer assessment of the optimal greenhouse design, it would be more appropriate to include the GHG emissions associated with greenhouse construction, provided that data is accessible.

5. Conclusions

This paper reports several greenhouse designs that were found to be efficient in terms of economic and environmental performance for both investors and policy makers across various price scenarios. The results

underscore the importance of tailoring greenhouse designs to local climate and market conditions, with specific recommendations for different regions. For example, the Venlo-type structure with glass cover is the most favorable choice for Jinshan, while a multi-tunnel structure appeared to be a more suitable for Langfang and Pingliang. Applying whitewash during summer is generally discouraged, except for in Langfang. Incorporating double-layer thermal screens in colder regions such as Langfang can be economically beneficial. In other cases, transparent thermal screen is a preferred choice to increase light use efficiency and improve yield.

The choice of lighting system, structure, thermal screen, and CO_2 dosing rate were among the most influential factors on operating income. When comparing LED to HPS lamps, LED lighting performs better in terms of both economic and environmental performance. However, it is crucial to note that lighting is the primary contributor to GHG emissions. As a result, the optimal designs identified either opt for no lighting or incorporated LED lamps with an intensity above 100 μmol m^{-2} s^{-1}, combined with a high CO_2 dosing rate. Low intensity lighting negatively affects both economic and environmental performance. The use of thermal screens, on the other hand, can effectively reduce GHG emissions.

Declaration of competing interest

This study is a part of the research project "Big Data Quantification and Modelling for Modern Agriculture in China" (Grant ID: 3183410600), which is financially supported by Lankuaikei Agriculture Developemt (Shanghai) Co., Ltd. The sponsor did not participate in study design, data collection, analysis, interpretation of data, and the writing of the manuscript, or any other decision that might affect the quality and objectivity of this manuscript.

Acknowledgement

We would like to acknowledge Kun Yang, Yuanpei Xie for providing climate setpoints; and Xiangming Chen, Jianfeng Dai, and Ying Ying for providing information on the initial investment costs of greenhouse design elements.

Appendix A. Lighting installation initial investment costs calculation

Table A1
Parameters for lighting installation initial investment costs calculation, depending on the lamp type and lighting intensity.

Item	Parameter	Unit	HPS	LED
Efficacy	η^{HPS}, η^{LED}	μmol J^{-1}	2.3	3.1
Lamp investment	I^{HPS}_{bulb}, I^{LED}_{lamp}	¥ W^{-1}	0.2 [a]	4.2 [b]
Lamp lifetime	n^{HPS}_{bulb}, n^{LED}_{lamp}	hours	10,000 [a]	35,000 [a]
Lamp maintenance	m^{HPS}_{lamp}, m^{LED}_{lamp}	%	1.0 [a]	0.5 [a]
Fixture investment	$I^{HPS}_{fixture}$	¥ W^{-1}	0.9 [a]	/
Fixture lifetime	$n^{HPS}_{fixture}$	years	7 [a]	/
Fixture maintenance	$m^{HPS}_{fixture}$	%	1.0	/
Cabling investment	I_{cable}	¥ W^{-1}	0.9 [a]	0.9 [a]
Cabling lifetime	n_{cable}	years	10 [a]	10 [a]
Cabling maintenance	m_{cable}	%	1.0 [a]	1.0 [a]
Initial investment costs per floor area				
50 μmol m^{-2} s^{-1}	I^{50}_{HPS}, I^{50}_{LED}	¥ m^{-2}	43.5	82.3
100 μmol m^{-2} s^{-1}	I^{100}_{HPS}, I^{100}_{LED}	¥ m^{-2}	87.0	164.5
150 μmol m^{-2} s^{-1}	I^{150}_{HPS}, I^{150}_{LED}	¥ m^{-2}	130.4	246.8
200 μmol m^{-2} s^{-1}	I^{200}_{HPS}, I^{200}_{LED}	¥ m^{-2}	173.9	329.9

a Raaphorst et al. (2019).
b X. Chen, personal communication, Nov 26, 2022.

Lighting installation consists of several components (bulbs, fixture, cabling for HPS; lamp and cabling for LED). The total investment costs of lighting installation (¥ m^{-2}), given a desired lighting intensity x (μmol m^{-2} s^{-1}), was calculated as:

$$I^{x}_{HPS} = \left(I^{HPS}_{bulb} + I^{HPS}_{fixture} + I_{cable}\right) * \frac{x}{\eta^{HPS}} \text{ for HPS lamps, and}$$

$$I^{x}_{LED} = \left(I^{LED}_{lamp} + I_{cable}\right) * \frac{x}{\eta^{LED}} \text{ for LED lamps}$$

The initial investment costs of each component was convert into the equivalent annuity cost (EAC), which is dependent on the lifetime (year) of the component. To calculated the lifetime of lamps, we divided the annual lighting hours, which is an output of the INTKAM-KASPRO model, by the lifetime (hour) of HPS bulb or LED lamp. The total EAC of lighting installation was give as:

$$EAC^{x}_{HPS} = EAC^{x}_{HPS-bulb} + EAC^{x}_{HPS-fixture} + EAC^{x}_{cable} \text{ for HPS lamps, and}$$

$$EAC^{x}_{LED} = EAC^{x}_{LED-Lamp} + EAC^{x}_{cable} \text{ for LED lamps}$$

Appendix B. Typical meteorological year climate data based on the ERA5 climate dataset from 2000 to 2020

To construct the typical meteorological year climate data based on the ERA5 dataset from 2000 to 2020, we followed the same method of typical meteorological year selection as in Song, F. et.al (2007), for the construction of Chinese Standard Weather Data.

The typical meteorological year climate data of each month is constituted by selecting a year between 2000 and 2020 with the most meteorological

representativeness of the month. Seven climate indicators contribute to the measure of meteorological representativeness. The indicators were assigned with different weights W_i according to their importance in meteorological representativeness, as shown in Table B1.

Table B1
Climate indicators and the corresponding weights for typical meteorological year selection.

Indicator	Weight W_i
Daily average temperature	2/16
Daily minimum temperature	1/16
Daily maximum temperature	1/16
Daily average sky temperature	1/16
Daily average relative humidity	2/16
Global radiation downwards	8/16
Daily average wind speed	1/16

The selecting process is described as below:

1. Calculate for each indicator the monthly mean values of each year from 2000 to 2020: $X_{i,m,y}$, where i denotes the climate indicator under consideration, m denotes the month indices and y denotes the year indices.
2. Calculate for each climate indicator i, the mean $\overline{X}_{i,m}$ and the standard deviation $S_{i,m}$ across multiple years.
3. Calculate for each indicator, the normalized monthly mean value of each year: $\eta_{i,m,y} = \frac{X_{i,m,y} - \overline{X}_{i,m}}{S_{i,m}}$.
4. Calculate for each month and each year, the weighted sum normalized absolute monthly mean of all climate indicators: $D_{m,y} = \sum_i W_i \bullet \left|\eta_{i,m,y}\right|$
5. Select for each month, the year with the smallest $\min_y D_{m,y}$.
6. Create the typical meteorological year data by appending the monthly climate data of the selected year, so for each month, the monthly data from the year with the smallest $D_{m,y}$become the same month data of the typical meteorological year.

Table B2
Selected years for each monthly for constructing the meteorological typical meteorological year climate dataset.

Month	Jinshan	Langfang	Weifang	Pingliang
January	2007	2008	2018	2019
February	2003	2015	2011	2015
March	2009	2004	2013	2014
April	2000	2001	2004	2009
May	2012	2015	2015	2015
June	2008	2016	2015	2011
July	2012	2013	2005	2009
August	2003	2010	2017	2000
September	2001	2020	2015	2015
October	2013	2008	2019	2011
November	2014	2001	2016	2008
December	2020	2019	2006	2015

Appendix C. Greenhouse climate management strategy

Table C1
Description of the greenhouse climate management strategy.

Parameter	Values	Description
$Tair_{\_heat}$ (day/night)	17 °C/14 °C	The heat is turned on when the indoor temperature (Tair) is below 17 °C during the day and 14 °C during the night.
$Pband_{\_heat}$	2 °C, 100 W m^{-2}, 400 W m^{-2}	When radiation (Iglob) is below 100 W m^{-2}, $Tair_{\_heat}$ is unaffected and above 400 W m^{-2} $Tair_{\_heat}$ increases by 2 °C. Between 100 and 400 W m^{-2}, $Tair_{\_heat}$ increment is linearly interpolated.
$Tout_{\_ThScr}$	10 °C if Iglob <100 W m^{-2}; 0 °C if Iglob <290 W m^{-2}	Thermal screen may be used when the outside temperature (Tout) is below 10 °C and radiation is above 100 W m^{-2}. When Tout goes below 0 °C, the thermal screen will be kept deployed until the radiation is above 290 W m^{-2}.
$Iglob_{\_ShScr}$	600 W m^{-2}, 800 W m^{-2}	The shading screen will be half closed when the radiation exceeds 600 W m^{-2} and fully closed when the radiation exceeds 800 W m^{-2}.
$Tair_{\_vent}$	16 °C/19 °C	Vent is open when Tair is above 19 °C during the day and 16 °C during the night.
$Pband_{\_vent}$	18 °C if Tout <6 °C, 4 °C if Tout >20 °C	$Pband_{vent}$ is a key parameter that controls how large the temperature excess has to be before the leeward vents are fully opened. The maximum opening of vents is 100%. When Tout is below 6 °C, the p-band is 18 °C; when Tout is above 20 °C, the p-band is 4 °C. The windward vents only open when the leeward vents are opened above 50%.
$Tair_{\_fan}$	2 °C	Fans will run on the maximum capacity when the difference between Tair and $Tair_{\_vent}$ excesses 2 °C. The air can be cooled down to 0.85 of the wet-bulb temperature. The outlet temperature is 1.5 °C above the average greenhouse temperature.
$RH_{\_fog}$	75%	Fogging system starts working when the indoor relative humidity (RH) drops below 75%.
$Pband_{\_fog}$	5%	Fogging system works at the maximum capacity when RH drops to 70%. The working capacity of fogging system is proportionally controlled from 0 to the maximum value.
$Time_{\_light\_on}$	00:00	Lamps are turned on at 00:00 after five weeks of planting; the maximum lighting hour is 18 h per day.

(*continued on next page*)

Table C1 (*continued*)

Parameter	Values	Description
$Iglob_{light\_off}$	400 W m^{-2}	Lamps are turned off when radiation is above 400 W m^{-2}.
$CO_{2\_setpoint}$ (day/night)	800 ppm/400 ppm	Extra CO_2 is applied is the indoor CO_2 concentration is below 800 ppm during the day, and 400 ppm during the night.
CO_{2_light}	1000 ppm	CO_2 setpoint set to 1000 ppm if lights are on.
CO_{2_vent}	100%, 20%; 50%, 40%; 25%, 75%	when the (leeward) vents are opened till 20%, the maximum CO2 dosing capacity is kept at 100%. When vents are opened till 40%, the CO2 dosing capacity is reduced to half its maximum capacity. When vents are opened above 70%, the dosing capacity stays at 25% of the maximum capacity.

Appendix D. Calculation of weighted average cost of capital (WACC)

Table D1
Calculation of weighted average cost of capital.

Cost of debt after tax shield (*CD*)	Rate	Source
Cost of debt (*Rd*)	5.5%	The People's Bank of China (2022), with the assumption of 20% floating rate on the 5-year Loan Prime Rate of 2022 (4.6%)
Marginal tax rate (*T*)	0.0%	Enterprise Income Tax Law of the People's Republic of China, article 27 (2007)
Cost of debt after tax shield	5.5%	
Cost of equity (*CE*)		
Risk free rate (*rfr*)	2.79%	China 10-year government bond yield (Ministry of Finance of the People's Republic of China, 2022)
Market risk premium of China (*rm*)	4.94%	(Damodaran, 2022a)
Beta for farming sector in China (β)	0.79	(Damodaran, 2022b)
Cost of equity	6.69%	Calculated
Capital structure	Ratio	
Debt (*D*)	50%	Authors' assumption
Equity (*E*)	50%	Authors' assumption
WACC	6.10%	Calculated

The discount rate *r* was calculated using the WACC method as follows:

$$r = WACC = \frac{D}{D+E} \bullet CD + \frac{E}{D+E} \bullet CE = \frac{D}{D+E} \bullet Rd \bullet (1-T) + \frac{E}{D+E} \bullet (rfr + \beta \bullet rm)$$

Damodaran, A. (2022a). Country Default Spread and Risk Premiums. https://pages.stern.nyu.edu/~adamodar/pc/datasets/ctryprem.xlsx Retrieved on 24th February 2022. Verified [April 2022].

Damodaran, A. (2022b). Levered and Unlevered Betas by Industry - China. https://pages.stern.nyu.edu/~adamodar/pc/datasets/totalbetaChina.xls Retrieved on 24th February 2022. Verified [April 2022].

Appendix E. Tomato and natural gas prices

Table E1
Monthly cherry tomato wholesale prices (¥ kg^{-1}) for 2021 (with 50% price premium).

Month	Jinshan[a]	Langfang	Weifang	Pingliang[b]
Jan	12.00	15.23	10.86	12.81
Feb	11.18	14.60	12.99	12.23
Mar	9.62	16.91	12.66	14.36
Apr	11.03	15.93	11.12	13.46
May	13.55	14.43	9.05	12.08
Jun	11.63	12.78	6.75	10.56
Jul	11.81	11.58	8.58	9.45
Aug	12.84	11.43	9.12	9.32
Sep	14.19	11.79	9.93	9.65
Oct	15.09	12.35	11.60	10.16
Nov	17.82	17.18	12.84	14.6
Dec	18.71	17.96	13.68	15.32

Source: National commercial information platform of agricultural product (nc.mofcom.gov.cn).

[a] Cherry tomato prices of Jiangsu province were used as proxies for Jinshan cherry tomato prices due to the lack of data.

[b] There are no price records for cherry tomato for Pingliang. Therefore, we estimated cherry tomato prices based on the price difference (92%) for globe tomatoes between Langfang and Pingliang. A transportation tarif of 1.2 ¥ kg^{-1} was applied for Pingliang, after consulting a greenhouse manager in Pingliang.

Table E2
Average monthly price (¥ m^{-3}) of natural gas from 2017 to 2022 for four regions.

Month	Jinshan	Langfang	Weifang	Pingliang
Jan	4.93	4.76	4.89	4.62
Feb	5.03	4.69	4.91	4.24
Mar	4.56	4.44	4.75	4.05
Apr	4.32	4.12	4.51	3.87
Oct	4.37	4.36	4.45	4.25
Nov	4.95	4.93	5.07	5.02
Dec	5.11	4.84	5.23	5.05

Source: Shanghai Petroleum and Natural Gas Exchange (2023) (https://www.shpgx.com/html/yhtrqsj.html).

Appendix F. Derivation of stakeholder weights

The values of stakeholders' weight for revenue increase $w^{R}_{stakeholder}$ and environmental impacts reduction $w^{GHG}_{stakeholder}$ used in this study were derived based on the unpublished results of Min et al. This appendix explains how the survey was conducted and how the weights were derived.

The survey aimed to elicit the relative importance of the six criteria, including *cost-benefit* and *environmental impacts* of greenhouse technologies, among multiple stakeholders in the Chinese greenhouse sector. The survey was designed according to the guidelines of the Best-Worst method, a multi-criteria decision-making method developed by Rezaei (2015) for addressing complex problems with multiple conflicting and subjective criteria. The survey was documented in Excel format.

We collected data from four groups of stakeholders: greenhouse growers, private investors, machinery and equipment suppliers, and agricultural policy makers in China. Ten respondents for each group were reached through snowball sampling. Specifically:

Investors were general managers or directors in a modern greenhouse company, located in Beijing, Shanghai, Shandong, Gansu, Jiangsu, Yunnan, and Guangdong provinces. The sample of growers and investors covers the stakeholders of major modern greenhouse companies in China.

Policy makers were recruited from the local ministry of agriculture, agricultural research institutes, extension centers, and quasi-commercialized state-owned enterprises. Policy makers were only included if they had participated in the design of local agricultural policy or had been involved in local greenhouse projects.

The surveys were conducted through a web conferencing platform and presented to the respondents through screen sharing. Each respondent was presented with an overview of all evaluation criteria. The respondents were first asked to identify which criteria they considered the most and least important when adopting (for investors) or promoting (for policy makers) digital or automation technology for greenhouse production. Respondents were then instructed to compare the remaining criteria to the selected most and least important criteria by assigning a number between 1 and 9. Throughout the survey interview, respondents were also asked to explain their choices.

A BWM solver was employed to calculate the optimal weights and the consistency ratio. In case of inconsistency, respondents were asked if they were willing to reconsider their judgement for the most inconsistent pair-wise comparison. Fig. F1 presents an example of a survey response that we collected.

the most important criterion	Cost-benefit

the least important criterion	Trialablity

Please evaluate the relative importance of [Cost-benefit] to other criteria (choose from 1 to 9)

Cost-benefit	1	2	9	3	3	6
	Cost-benefit	Environmental	Trialablity	Observability	Complexity	Compatibility

Please evaluate the relative importance of other criteria to [Trialablity] (choose from 1 to 9)

	Cost-benefit	Environmental	Trialablity	Observability	Complexity	Compatibility
Trialablity	9	6	1	4	4	2

Scale of importance (1-9)

1: **Equal** importance
2: Somewhat between Equal and Moderate
3: **Moderately** more important
4: Somewhat between Moderate and Strong
5: **Strongly** more important than
6: Somewhat between Strong and Very strong
7: **Very strongly** important than
8: Somewhat between Very strong and Absolute
9: **Absulutly** more important

Your weights

Weights	Cost-benefit	Environmental	Trialablity	Observability	Complexity	Compatibility
	0.39	0.21	0.04	0.14	0.14	0.07

Consistency check

Consistency ratio	0.0417	Consistency check passed
Consistency threshold	0.3337	

Fig. F1. Example of a survey response.

After deriving the optimal weights for each respondent, we calculated the weight for each stakeholder group by taking the arithmetic mean of the optimal weights for individual respondents within the stakeholder group. The values for $w^{R}_{stakeholder}$ and $w^{GHG}_{stakeholder}$ were then calculated as:

$$w^{R}_{stakeholder} = \frac{w^{cost-benefit}_{stakeholder}}{w^{cost-benefit}_{stakeholder} + w^{environmental}_{stakeholder}}$$

$$w^{GHG}_{stakeholder} = \frac{w^{environmental}_{stakeholder}}{w^{cost-benefit}_{stakeholder} + w^{environmental}_{stakeholder}}$$

Appendix G. Categorical regression results: the effect of individual design element on operating income and GHG emissions

Table G1
Categorical regression results: the relationship between design element choice and the annual operating income (baseline scenario).

Variable	Design element choice	Jinshan	Langfang	Weifang	Pingliang
Structure_A	*Multi- tunnel, 1 vent 10 m^{-2}*	*baseline choice*			
Structure_B	Multi- tunnel, 1 vent 20 m^{-2}	24.7 (*0.3*)	34.9 (*0.4*)	26.2 (*0.3*)	36.3 (*0.5*)
Structure_C	Multi- tunnel, 1 vent 30 m^{-2}	39.1 (*0.2*)	52.0 (*0.3*)	41.7 (*0.3*)	55.0 (*0.5*)
Structure_D	Venlo, 1 vent 10 m^{-2}	8.4 (*0.3*)	7.7 (*0.5*)	5.3 (*0.4*)	10.6 (*0.7*)
Structure_E	Venlo, 1 vent 20 m^{-2}	33.5 (*0.3*)	41.8 (*−0.4*)	33.6 (*0.4*)	44.5 (*0.6*)
Structure_F	Venlo, 1 vent 30 m^{-2}	46.2 (*0.3*)	55.2 (*0.4*)	46.1 (*0.3*)	59.8 (*0.6*)
Cover_A	*Single PE film*	*baseline choice*			
Cover_B	Double PE film	−3.5 (*0.2*)	−5.1 (*0.2*)	0.7 (*0.2*)	7.0 (*0.4*)
Cooling_A	*No cooling*	*baseline choice*			
Cooling_B	Fogging: 200 g h^{-1} m^{-2}	−6.5 (*0.2*)	5.1 (*0.3*)	−4.9 (*0.2*)	−4.4 (*0.4*)
Cooling_C	Fogging: 300 g h^{-1} m^{-2}	−7.0 (*0.2*)	5.6 (*0.3*)	−5.7 (*0.2*)	−5.4 (*0.4*)
Cooling_D	Fogging: 400 g h^{-1} m^{-2}	−10.1 (*0.2*)	2.3 (*0.3*)	−9.0 (*0.3*)	−8.4 (*0.4*)
Cooling_E	Pad and fan: 60 m^3 h^{-1} m^{-2}	−42.2 (*0.3*)	−17.4 (*0.4*)	−22.2 (*0.3*)	−53.5 (*0.7*)
Cooling_F	Pad and fan: 90 m^3 h^{-1} m^{-2}	−54.1 (*0.3*)	−25.0 (*0.4*)	−32.6 (*0.3*)	−65.1 (*0.7*)
Cooling_G	Pad and fan: 120 m^3 h^{-1} m^{-2}	−64.6 (*0.3*)	−33.4 (*0.4*)	−40.8 (*0.4*)	−75.1 (*0.7*)
Heating_A	*1.16 MW ha^{-1}*	*baseline choice*			
Heating_B	1.74 MW ha^{-1}	−0.4 (*0.2*)	0.6 (*0.2*)	−0.5 (*0.2*)	1.4 (*0.3*)
Heating_C	2.32 MW ha^{-1}	−0.1 (*0.2*)	1.0 (*0.2*)	0.1 (*0.2*)	1.4 (*0.3*)
Thermal_screen_A	*No thermal screens*	*baseline choice*			
Thermal_screen_B	Transparent	40.5 (*0.3*)	59.0 (*0.4*)	53.8 (*0.3*)	73.0 (*0.6*)
Thermal_screen_C	Non-transparent	23.8 (*0.3*)	35.5 (*0.4*)	31.2 (*0.4*)	46.8 (*0.7*)
Thermal_screen_D	One side black	22.5 (*0.3*)	39.0 (0.4)	33.8 (*0.4*)	47.6 (*0.7*)
Thermal_screen_E	Double-layer	32.9 (*0.3*)	57.4 (0.4)	49.8 (*0.3*)	70.0 (*0.7*)
Shade_screen_A	*No shade screens*	*baseline choice*			
Shading_screen_B	36% shading	−4.4 (*0.2*)	3.4 (0.2)	0.5 (*0.2*)	1.0 (*0.4*)
Shading_screen_C	45% shading	−8.6 (*0.2*)	−4.0 (0.3)	−4.8 (*0.2*)	−4.5 (*0.4*)
Shading_screen_D	56% shading	−9.1 (*0.2*)	−3.6 (0.3)	−5.1 (*0.2*)	−4.4 (*0.4*)
Light_A	*No supplemental lighting*	*baseline choice*			
Light_B	HPS, 50 μmol m^{-2} s^{-1}	−25.4 (*1.1*)	−8.8 (2.1)	−79.2 (*2.1*)	57.7 (*4.4*)
Light_C	HPS, 100 μmol m^{-2} s^{-1}	−49.9 (*1.1*)	−8.7 (2.1)	−92.4 (*1.9*)	28.0 (*3.9*)
Light_D	HPS, 150 μmol m^{-2} s^{-1}	36.7 (*0.8*)	154.4 (1.4)	−3.9 (*1.3*)	229.4 (*2.1*)
Light_E	HPS, 200 μmol m^{-2} s^{-1}	57.6 (*0.6*)	186.1 (1.0)	17.1 (*1.1*)	252.3 (*1.3*)
Light_F	LED, 50 μmol m^{-2} s^{-1}	−13.9 (*1.0*)	−3.6 (1.9)	−74.1 (*1.7*)	42.1 (*3.9*)
Light_G	LED, 100 μmol m^{-2} s^{-1}	−27.8 (*1.0*)	−9.5 (2.0)	−82.8 (*1.6*)	28.8 (*3.3*)
Light_H	LED, 150 μmol m^{-2} s^{-1}	72.1 (*0.8*)	159.6 (1.9)	10.4 (*1.2*)	224.8 (*2.6*)
Light_I	LED, 200 μmol m^{-2} s^{-1}	97.3 (*0.5*)	200.2 (0.7)	33.2 (*0.6*)	253.1 (*1.3*)
CO_2_A	*No CO_2 enrichment*	*baseline choice*			
CO_2_B	50 kg CO_2 ha^{-1} h^{-1}	−16.8 (*1.0*)	−26.8 (1.9)	−85.7 (*1.4*)	15.2 (*3.4*)
CO_2_C	100 kg CO_2 ha^{-1} h^{-1}	−18.9 (*0.9*)	−27.1 (1.2)	−87.5 (*1.1*)	13.4 (*2.5*)
CO_2_D	150 kg CO_2 ha^{-1} h^{-1}	−18.6 (*0.9*)	−32.3 (1.0)	−89.7 (*0.9*)	7.7 (*1.7*)
CO_2_E	200 kg CO_2 ha^{-1} h^{-1}	−19.3 (*0.8*)	−33.5 (1.0)	−89.3 (*0.8*)	6.0 (*1.4*)
Whitewash_A	*No whitewash*	*baseline choice*			
Whitewash_B	50% transmission	−4.6 (*0.1*)	2.3 (0.2)	−5.6 (*0.2*)	−8.8 (*0.3*)
light_B*CO2_B		14.3 (*1.7*)	29.7 (3.3)	83.3 (*2.8*)	−39.2 (*6.1*)
light_B*CO2_C		13.1 (*1.6*)	23.4 (2.8)	82.1 (*2.5*)	−38.5 (*5.8*)
light_B*CO2_D		11.2 (*1.6*)	30.9 (2.5)	82.0 (*2.4*)	−36.0 (*4.9*)
light_B*CO2_E		7.7 (*1.5*)	28.9 (2.4)	82.4 (*2.4*)	−41.5 (*4.7*)
light_C*CO2_B		16.9 (*1.8*)	27.7 (3.3)	86.9 (*2.8*)	−22.9 (*6.1*)
light_C*CO2_C		15.1 (*1.6*)	24.8 (2.7)	85.3 (*2.4*)	−22.5 (*5.3*)
light_C*CO2_D		10.9 (*1.6*)	27.8 (2.5)	86.3 (*2.2*)	−19.7 (*4.6*)
light_C*CO2_E		9.9 (*1.5*)	28.2 (2.4)	83.6 (*2.2*)	−22.8 (*4.2*)
light_D*CO2_B		23.7 (*1.4*)	42.5 (2.6)	91.9 (*2.0*)	17.5 (*4.4*)
light_D*CO2_C		26.3 (*1.3*)	42.2 (2.0)	95.8 (*1.8*)	35.4 (*3.5*)
light_D*CO2_D		25.5 (*1.3*)	52.8 (*1.8*)	100.1 (*1.7*)	52.9 (*2.8*)
light_D*CO2_E		24.9 (*1.2*)	55.9 (*1.8*)	98.4 (*1.6*)	62.1 (*2.6*)
light_E*CO2_B		25.9 (*1.2*)	58.9 (*2.2*)	99.6 (*1.9*)	25.0 (*3.6*)
light_E*CO2_C		33.2 (*1.0*)	75.3 (*1.6*)	108.7 (*1.6*)	52.1(*2.7*)
light_E*CO2_D		35.3 (*1.0*)	87.8 (*1.4*)	112.2 (*1.4*)	75.6 (*1.9*)
light_E*CO2_E		37.1 (*1.0*)	94.5 (*1.4*)	113.3 (*1.4*)	87.1 (*1.6*)
light_F*CO2_B		14.8 (*1.7*)	28.1 (*3.1*)	84.7 (*2.5*)	−14.4 (*5.9*)
light_F*CO2_C		13.5 (*1.5*)	25.5 (*2.5*)	81.1 (*2.2*)	−22.1 (*5.3*)
light_F*CO2_D		10.8 (*1.5*)	31.5 (*2.4*)	82.9 (*2.1*)	−16.7 (*4.5*)
light_F*CO2_E		7.4 (*1.4*)	29.1 (*2.3*)	80.6 (*2.0*)	−20.7 (*4.2*)
light_G*CO2_B		18.2 (*1.7*)	33.7 (*3.1*)	86.6 (*2.4*)	(−0.8) (*5.6*)
light_G*CO2_C		17.0 (*1.6*)	31.4 (*2.7*)	85.6 (*2.2*)	−13.4 (*4.6*)
light_G*CO2_D		12.4 (*1.5*)	36.2 (*2.5*)	87.1 (*2.0*)	−9.1 (*4.1*)
light_G*CO2_E		10.9 (*1.5*)	37.7 (*2.4*)	84.1 (*1.9*)	−12.1 (*3.6*)
light_H*CO2_B		21.9 (*1.4*)	43.3 (*2.9*)	92.4 (*2.0*)	11.6 (*4.8*)
light_H*CO2_C		24.7 (*1.3*)	53.9 (*2.4*)	97.7 (*1.7*)	36.9 (*4.0*)
light_H*CO2_D		25.4 (*1.2*)	61.6 (*2.2*)	101.9 (*1.5*)	54.3 (*3.2*)
light_H*CO2_E		25.0 (*1.2*)	64.8 (*2.1*)	100.7 (*1.5*)	63.8 (*3.0*)

(*continued on next page*)

Table G1 (*continued*)

Variable	Design element choice	Jinshan	Langfang	Weifang	Pingliang
light_I*CO2_B		26.7 (*1.1*)	57.6 (*2.0*)	101.9 (*1.5*)	24.6 (*3.7*)
light_I*CO2_C		34.6 (*1.0*)	75.2 (*1.3*)	110.9 (*1.2*)	49.3 (*2.8*)
light_I*CO2_D		36.8 (*0.9*)	88.7 (*1.2*)	115.7 (*1.0*)	71.1 (*2.0*)
light_I*CO2_E		38.3 (*0.9*)	94.0 (*1.1*)	116.2 (*0.9*)	81.0 (*1.7*)

Note: Standard errors of the coefficients were given in brackets. The insignificant coefficients are underlined, all other coefficients are significant at 0.05 level.

Table G2
Categorical regression results: the relationship between design element choice and greenhouse gas emissions.

Variable	Design element choice	Jinshan	Langfang	Weifang	Pingliang
Structure_A	*Multi- tunnel, 1 vent 10 m^{-2}*	*baseline choice*			
Structure_B	Multi- tunnel, 1 vent 20 m^{-2}	−8.0 (*0.1*)	−9.1 (*0.2*)	−8.5 (*0.1*)	−7.1 (*0.1*)
Structure_C	Multi- tunnel, 1 vent 30 m^{-2}	−12.6 (*0.1*)	−14.7 (*0.1*)	−13.7 (*0.1*)	−11.3 (*0.1*)
Structure_D	Venlo, 1 vent 10 m^{-2}	−5.8 (*0.1*)	−5.1 (*0.2*)	−5.1 (*0.2*)	−5.0 (*0.2*)
Structure_E	Venlo, 1 vent 20 m^{-2}	−13.2 (*0.1*)	−13.5 (*0.2*)	−13.1 (*0.1*)	−11.4 (*0.1*)
Structure_F	Venlo, 1 vent 30 m^{-2}	−17.5 (*0.1*)	−18.4 (*0.2*)	−17.5 (*0.1*)	−14.6 (*0.1*)
Cover_A	*Single PE film*	*baseline choice*			
Cover_B	Double PE film	6.9 (*0.0*)	10.8 (*0.1*)	9.0 (*0.1*)	7.0 (*0.1*)
Cooling_A	*No cooling*	*baseline choice*			
Cooling_B	Fogging: 200 g h^{-1} m^{-2}	0.0 (*0.1*)	0.5 (*0.1*)	0.1 (*0.1*)	0.1 (*0.1*)
Cooling_C	Fogging: 300 g h^{-1} m^{-2}	0.1 (*0.1*)	0.5 (*0.1*)	0.0 (*0.1*)	0.0 (*0.1*)
Cooling_D	Fogging: 400 g h^{-1} m^{-2}	0.1 (*0.1*)	0.5 (*0.1*)	0.0 (*0.1*)	0.2 (*0.1*)
Cooling_E	Pad and fan: 60 m^3 h^{-1} m^{-2}	10.2 (*0.1*)	12.0 (*0.2*)	11.1 (*0.1*)	10.3 (*0.2*)
Cooling_F	Pad and fan: 90 m^3 h^{-1} m^{-2}	15.0 (*0.1*)	18.4 (*0.2*)	16.7 (*0.1*)	15.0 (*0.2*)
Cooling_G	Pad and fan: 120 m^3 h^{-1} m^{-2}	20.1 (*0.1*)	24.7 (*0.2*)	22.8 (*0.2*)	20.0 (*0.2*)
Heating_A	*1.16 MW ha^{-1}*	*baseline choice*			
Heating_B	1.74 MW ha^{-1}	0.4 (*0.0*)	1.2 (*0.1*)	1.2 (*0.1*)	0.2 (*0.1*)
Heating_C	2.32 MW ha^{-1}	0.5 (*0.0*)	1.0 (*0.1*)	1.0 (*0.1*)	0.4 (*0.1*)
Thermal_screen_A	*No thermal screens*	*baseline choice*			
Thermal_screen_B	Transparent	−21.4 (*0.1*)	−27.1 (*0.2*)	−27.1 (*0.1*)	−27.3 (*0.1*)
Thermal_screen_C	Non-transparent	−14.8 (*0.1*)	−7.2 (*0.2*)	−11.7 (*0.2*)	−13.5 (*0.2*)
Thermal_screen_D	One side black	−14.9 (*0.1*)	−9.7 (*0.2*)	−13.6 (*0.2*)	−13.1 (*0.2*)
Thermal_screen_E	Double-layer	−19.8 (*0.1*)	−17.4 (*0.2*)	−20.8 (*0.1*)	−22.1 (*0.1*)
Shade_screen_A	*No shade screens*	*baseline choice*			
Shading_screen_B	36% shading	−2.5 (*0.0*)	−3.0 (*0.1*)	−3.3 (*0.1*)	0.0 (*0.1*)
Shading_screen_C	45% shading	−1.4 (*0.1*)	−0.3 (*0.1*)	−1.0 (*0.1*)	0.9 (*0.1*)
Shading_screen_D	56% shading	−1.4 (*0.1*)	−0.4 (*0.1*)	−1.0 (*0.1*)	1.0 (*0.1*)
Light_A	*No supplemental lighting*	*baseline choice*			
Light_B	HPS, 50 μmol m^{-2} s^{-1}	115.9 (*0.1*)	156.5 (*0.4*)	147.1 (*0.3*)	114.6 (*0.3*)
Light_C	HPS, 100 μmol m^{-2} s^{-1}	155.4 (*0.1*)	211.5 (*0.4*)	193.7 (*0.3*)	151.4 (*0.3*)
Light_D	HPS, 150 μmol m^{-2} s^{-1}	187.5 (*0.1*)	257.6 (*0.3*)	228.2 (*0.3*)	180.6 (*0.3*)
Light_E	HPS, 200 μmol m^{-2} s^{-1}	210.7 (*0.1*)	284.4 (*0.3*)	248.4 (*0.2*)	200.5 (*0.2*)
Light_F	LED, 50 μmol m^{-2} s^{-1}	99.2 (*0.1*)	133.8 (*0.4*)	128.2 (*0.3*)	101.1 (*0.3*)
Light_G	LED, 100 μmol m^{-2} s^{-1}	123.1 (*0.1*)	166.3 (*0.3*)	156.3 (*0.3*)	1227. (*0.3*)
Light_H	LED, 150 μmol m^{-2} s^{-1}	142.1 (*0.1*)	194.7 (*0.3*)	177.4 (*0.3*)	140.0 (*0.3*)
Light_I	LED, 200 μmol m^{-2} s^{-1}	155.8 (0.1)	211.0 (0.2)	189.9 (0.2)	151.7 (0.2)
CO_2_A	*No CO_2 enrichment*	*baseline choice*			
CO_2_B	50 kg CO_2 ha^{-1} h^{-1}	0.0 (0.1)	0.4 (0.2)	0.3 (0.1)	0.1 (0.2)
CO_2_C	100 kg CO_2 ha^{-1} h^{-1}	−0.1 (0.1)	0.6 (0.2)	0.4 (0.1)	0.3 (0.2)
CO_2_D	150 kg CO_2 ha^{-1} h^{-1}	0.0 (0.1)	0.3 (0.2)	0.5 (0.1)	0.2 (0.1)
CO_2_E	200 kg CO_2 ha^{-1} h^{-1}	0.1 (0.1)	0.6 (0.2)	0.4 (0.1)	0.5 (0.1)
Whitewash_A	*No whitewash*	*baseline choice*			
Whitewash_B	50% transmission	3.5 (0.0)	7.76 (0.0)	6.78 (0.0)	5.80 (0.0)

Note: Standard errors of the coefficients were given in brackets. The insignificant coefficients are underlined, all other coefficients are significant at 0.05 level.

Appendix H. Supplementary Data

Python code for performance evaluation of greenhouse designs and the implementation of genetic algorithm are available as supplementary materials at https://github.com/Xinyuan-wur/greenhouse-design-optimization.

References

Aytug, H., Khouja, M., Vergara, F.E., 2003. Use of genetic algorithms to solve production and operations management problems: a review. Int. J. Prod. Res. 41 (17), 3955–4009. https://doi.org/10.1080/00207540310001626319.

Chung, Y.H., Färe, R., Grosskopf, S., 1997. Productivity and undesirable outputs: a directional distance function approach. *J. Environ. Manage.* 51 (3), 229–240. https://doi.org/10.1006/jema.1997.0146.

De Zwart, H.F., 1996. Analyzing Energy-Saving Potentials in Greenhouse Cultivation Using a simulation Model. [Doctoral dissertation, Wageningen University]. https://edepot.wur.nl/195238.

Diaz-Gomez, P.A., Hougen, D.F., 2007. Initial Population for Genetic Algorithms: A Metric Approach. IEEE Games Entertainment Media Conference.

Eremeev, A.V., 1999. A genetic algorithm with a non-binary representation for the set covering problem. In: Operations Research Proceedings 1998. Springer, Berlin, Heidelberg, pp. 175–181.

Esmaeli, H., Roshandel, R., 2020. Optimal design for solar greenhouses based on climate conditions. Renew. Energy 145, 1255–1265. https://doi.org/10.1016/j.renene.2019.06.090.

Gen, M., Cheng, R., 1999. Genetic Algorithms and Engineering Optimization, vol. 7. John Wiley & Sons.

Harik, G.R., Lobo, F.G., 1999. A parameter-less genetic algorithm. Proceedings of the Genetic and Evolutionary Computation Conference 258–267.

Heuvelink, E., Li, T., Dorais, M., 2018. Crop growth and yield. In: Heuvelink, E. (Ed.), Tomatoes, 2nd ed. Cabi, pp. 89–135. https://doi.org/10.1079/9781780641935.0000.
Holland, J.H., 1992. Adaptation in Natural and Artificial Systems: An Introductory Analysis with Applications to Biology, Control, and Artificial Intelligence. MIT press.
IPCC, 2007. In: Eggleston, H.S., Buendia, L., Miwa, K., Ngara, T., Tanabe, K. (Eds.), 2006 IPCC Guidelines for National Greenhouse gas Inventories (Vol. 2): Chapter 2-Stationary Combustion. IGES, Japan. https://www.ipcc-nggip.iges.or.jp/public/2006gl/vol2.html.
IPCC, 2014. In: Core Writing Team, Pachauri, R.K., Meyer, L.A. (Eds.), Climate Change 2014: Synthesis Report, Contribution of Working Groups I, II and III to the Fifth Assessment Report of the Intergovernmental Panel on Climate Change. IPCC, Geneva, Switzerland. https://www.ipcc.ch/site/assets/uploads/2018/02/SYR_AR5_FINAL_full.pdf.
Lee, L.H., Chew, E.P., Teng, S., Chen, Y., 2008. Multi-objective simulation-based evolutionary algorithm for an aircraft spare parts allocation problem. Eur. J. Oper. Res. 189 (2), 476–491. https://doi.org/10.1016/j.ejor.2007.05.036.
Lehmann, N., Finger, R., Klein, T., Calanca, P., Walter, A., 2013. Adapting crop management practices to climate change: modeling optimal solutions at the field scale. Agr. Syst. 117, 55–65. https://doi.org/10.1016/j.agsy.2012.12.011.
Lin, R.C., Sir, M.Y., Pasupathy, K.S., 2013. Multi-objective simulation optimization using data envelopment analysis and genetic algorithm: specific application to determining optimal resource levels in surgical services. Omega 41 (5), 881–892. https://doi.org/10.1016/j.omega.2012.11.003.
Los, E., Gardebroek, C., Huirne, R., 2021. Firm-specific responses to energy policies in Dutch horticulture. Eur. Rev. Agric. Econ. 48 (2), 362–384. https://doi.org/10.1093/erae/jbab004.
Luo, W., Stanghellini, C., Dai, J., Wang, X., Feije De Zwart, H., Bu, C., 2005. Simulation of greenhouse management in the subtropics, part II: scenario study for the summer season. Biosyst. Eng. 90 (4), 433–441. https://doi.org/10.1016/j.biosystemseng.2004.12.002.
Marcelis, L.F.M., Elings, A., De Visser, P.H.B., Heuvelink, E., 2008. Simulating growth and development of tomato crop. In: International Symposium on Tomato in the Tropics, 821, pp. 101–110. https://doi.org/10.17660/ActaHortic.2009.821.10.
Mayer, D.G., Belward, J.A., Widell, H., Burrage, K., 1999. Survival of the fittest—genetic algorithms versus evolution strategies in the optimization of systems models. Agr. Syst. 60 (2), 113–122. https://doi.org/10.1016/S0308-521X(99)00022-0.
Mendes, J.M., Oliveira, P.M., dos Santos, F.N., Morais dos Santos, R., 2019. Nature inspired metaheuristics and their applications in agriculture: A short review. In: Oliveira, P.M., Novais, P., Reis, L.P. (Eds.), EPIA Conference on Artificial Intelligence. Springer International Publishing, Cham, pp. 167–179. https://doi.org/10.1007/978-3-030-30241-2.
Meyer-Aurich, A., Jubaer, H., Scholz, L., Ziegler, T., Daalgard, T., Yli-Kojola, H., Esala, J., Mikkola, H., Rajaniemi, M., Jokiniemi, T., Ahokas, J., Golaszewski, J., Stolarski, M., Brodzinski, Z., Myhan, R., Olba-Ziety, E., de Visser, C., van der Voort, M., Stanghellini, C., Ellen, H., Klop, A., Wemmenhove, H., Baptista, F., Murcho, D., Silva, L.L., Silva, J.R., Peça, J.O., Louro, M., Marques, C., Mistriotis, A., Balafoutis, A., Panagakis, P., Briassoulis, D., 2012. Economic and environmental analysis of energy efficiency measures in agriculture. Case studies and trade offs. AGREE Project Deliverable 3 (1), 157 p. https://edepot.wur.nl/278553.
Min, X., Sok, J., Elings, A., Oude Lansink, A., 2022. Economic feasibility of glasshouse tomato production in China—A bio-economic stochastic modelling approach. NJAS: Impact in Agricultural and Life Sciences 94 (1), 156–183. https://doi.org/10.1080/27685241.2022.2135390.
Ministry of Agriculture of the People''s Republic of China (MOA), 2018. Present situation of and advice on protected horticulture development in China. http://new.zhiguker.com/index/article/detail?id=24762&nav=0 (Retrieved on 17th March, 2022 Verified [April, 2023]).
Montero, J.I., Zhang, Y., Yang, Q., Ke, X., 2019. Advances in greenhouse design. In: Marcelis, L.F., Heuvelink, E. (Eds.), Achieving Sustainable Greenhouse Cultivation. Burleigh Dodds Science Publishing, pp. 17–52. https://doi.org/10.1201/9780429266744.
Naseer, M., Persson, T., Righini, I., Stanghellini, C., Maessen, H., Verheul, M.J., 2021. Bio-economic evaluation of greenhouse designs for seasonal tomato production in Norway. Biosystems Engineering 212, 413–430. https://doi.org/10.1016/j.biosystemseng.2021.11.005.
Naseer, M., Persson, T., Righini, I., Stanghellini, C., Maessen, H., Ruoff, P., Verheul, M.J., 2022. Bioeconomic evaluation of extended season and year-round tomato production in Norway using supplemental light. Agr. Syst. 198, 103391 https://doi.org/10.1016/j.agsy.2022.103391.
Notte, G., Pedemonte, M., Cancela, H., Chilibroste, P., 2016. Resource allocation in pastoral dairy production systems: evaluating exact and genetic algorithms approaches. Agr. Syst. 148, 114–123. https://doi.org/10.1016/j.agsy.2016.07.009.
Price, W.L., 1977. A controlled random search procedure for global optimisation. Comput. J. 20 (4), 367–370. https://doi.org/10.1093/comjnl/20.4.367.
Qu, S., Liang, S., Xu, M., 2017. CO_2 emissions embodied in interprovincial electricity transmissions in China. Environ. Sci. Technol. 51 (18), 10893–10902. https://doi.org/10.1021/acs.est.7b01814.
Raaphorst, M.G., Benninga, J., Eveleens, B.A., 2019. Quantitative Information on Dutch Greenhouse Horticulture 2019. Report WPR-898, 26th ed. (Bleiswijk, the Netherlands).
Rezaei, Jafar, 2015. Best-worst multi-criteria decision-making method. Omega. 53, 49–57. https://doi.org/10.1016/j.omega.2014.11.009.
Shadkam, E., Bijari, M., 2017. Multi-objective simulation optimization for selection and determination of order quantity in supplier selection problem under uncertainty and quality criteria. Int. J. Adv. Manuf. Technol. 93, 161–173. https://doi.org/10.1007/s00170-015-7986-1.
Song, F., Zhu, Q., Wu, R., Jiang, Y., Xiong, A., Wang, B., Zhu, Y., Li, Q., 2007. Meteorological data set for building thermal environment analysis of China. In: The 10th international building performance simulation association conference and exhibition, Beijing, China; 2007. https://www.aivc.org/node/34982.
Sun, J., Gao, H., Tian, J., Wang, J., Du, C., Guo, S., 2019. Development status and trends of protected horticulture in China. Journal of Nanjing Agricultural University 42 (4), 594–604. https://doi.org/10.7685/jnau.201810027.
Torrellas, M., Antón, A., Ruijs, M., Victoria, N.G., Stanghellini, C., Montero, J.I., 2012. Environmental and economic assessment of protected crops in four European scenarios. J. Clean. Prod. 28, 45–55. https://doi.org/10.1016/j.jclepro.2011.11.012.
van Henten, E.J., Bakker, J.C., Marcelis, L.F.M., Van't Ooster, A., Dekker, E., Stanghellini, C., Vanthoor, B., Van Randeraat, B., Westra, J., 2006. The adaptive greenhouse an integrated systems approach to developing protected cultivation systems. Acta Hortic. 718, 399–406. https://doi.org/10.17660/ActaHortic.2006.718.46.
Vanthoor, B.H.E., Stigter, J.D., van Henten, E.J., Stanghellini, C., de Visser, P.H.B., Hemming, S., 2012. A methodology for model-based greenhouse design: part 5, greenhouse design optimisation for southern-Spanish and Dutch conditions. Biosystems Engineering 111 (4), 350–368. https://doi.org/10.1016/j.biosystemseng.2012.01.005.
Villalba, D., Díez-Unquera, B., Carrascal, A., Bernués, A., Ruiz, R., 2019. Multi-objective simulation and optimisation of dairy sheep farms: exploring trade-offs between economic and environmental outcomes. Agr. Syst. 173, 107–118. https://doi.org/10.1016/j.agsy.2019.01.011.
Wang, M., 2020. The market situation of snack tomato in China. Agricultural Engineering Technology (Greenhouse Horticulture) 40 (31), 34–37. https://kns.cnki.net/kcms/detail/detail.aspx?doi=10.16815/j.cnki.11-5436/s.2020.31.006.
Wang, J., Li, S., Guo, S., Ma, C., Wang, J., Jin, S., 2014. Simulation and optimization of solar greenhouses in northern Jiangsu Province of China. Energ. Buildings 78, 143–152. https://doi.org/10.1016/j.enbuild.2014.04.006.
West, J., 2019. Multi-criteria evolutionary algorithm optimization for horticulture crop management. Agr. Syst. 173, 469–481. https://doi.org/10.1016/j.agsy.2019.03.016.
Whittaker, G., Confesor Jr., R., Griffith, S.M., Färe, R., Grosskopf, S., Steiner, J.J., Banowetz, G.M., 2009. A hybrid genetic algorithm for multiobjective problems with activity analysis-based local search. European Journal of Operational Research 193 (1), 195–203. https://doi.org/10.1016/j.ejor.2007.10.050.
Zbigniew, M., 1996. Genetic algorithms+ data structures= evolution programs. In: Computational Statistics. Springer-Verlag, pp. 372–373.
Zhang, X., Qiu, H., Huang, Z., 2010. Apple and tomato chains in China and the EU (Report No. 2010-019). LEI Wageningen. ISBN: 978-90-8615-427-2. Available at. https://edepot.wur.nl/142956.
Zhou, D., Meinke, H., Wilson, M., Marcelis, L.F., Heuvelink, E., 2021. Towards delivering on the sustainable development goals in greenhouse production systems. Resour. Conserv. Recycl. 169, 105379 https://doi.org/10.1016/j.resconrec.2020.105379.

Data reference

Hersbach, H., Bell, B., Berrisford, P., Biavati, G., Horányi, A., Muñoz Sabater, J., Nicolas, J., Peubey, C., Radu, R., Rozum, I., Schepers, D., Simmons, A., Soci, C., Dee, D., Thépaut, J.-N., 2018. ERA5 hourly data on single levels from 1959 to present. Copernicus Climate Change Service (C3S) Climate Data Store (CDS). Accessed on January, 2022. https://doi.org/10.24381/cds.adbb2d47.
Shanghai Petroleum and Natural Gas Exchange, 2023. Liquid Natural Gas Prices. https://www.shpgx.com/html/yhtrqsj.html. Retrieved on 6th Feburay, 2022. Verified.